CHAPTER 3

Carbon Cycle

I. INTRODUCTION

Carbon is a constituent of all terrestrial life. Carbon begins its cycle through forest ecosystems when plants assimilate atmospheric CO_2 through photosynthesis into reduced sugars (Fig. 3.1). Usually about half the gross photosynthetic products produced (GPP) are expended by plants in autotrophic respiration (R_a) for the synthesis and maintenance of living cells, releasing CO_2 back into the atmosphere. The remaining carbon products (GPP − R_a) go into net primary production (NPP): foliage, branches, stems, roots, and plant reproductive organs. As plants shed leaves and roots, or are killed, the dead organic matter forms detritus, a substrate that supports animals and microbes, which through their heterotrophic metabolism (R_h) release CO_2 back into the atmosphere. On an annual basis, undisturbed forest ecosystems generally show a small net gain in carbon exchange with the atmosphere. This represents net ecosystem production (NEP). The ecosystem may lose carbon if photosynthesis is suddenly reduced or when organic materials are removed as a result of disturbance (Chapter 6). Soil humus represents the major accumulation of carbon

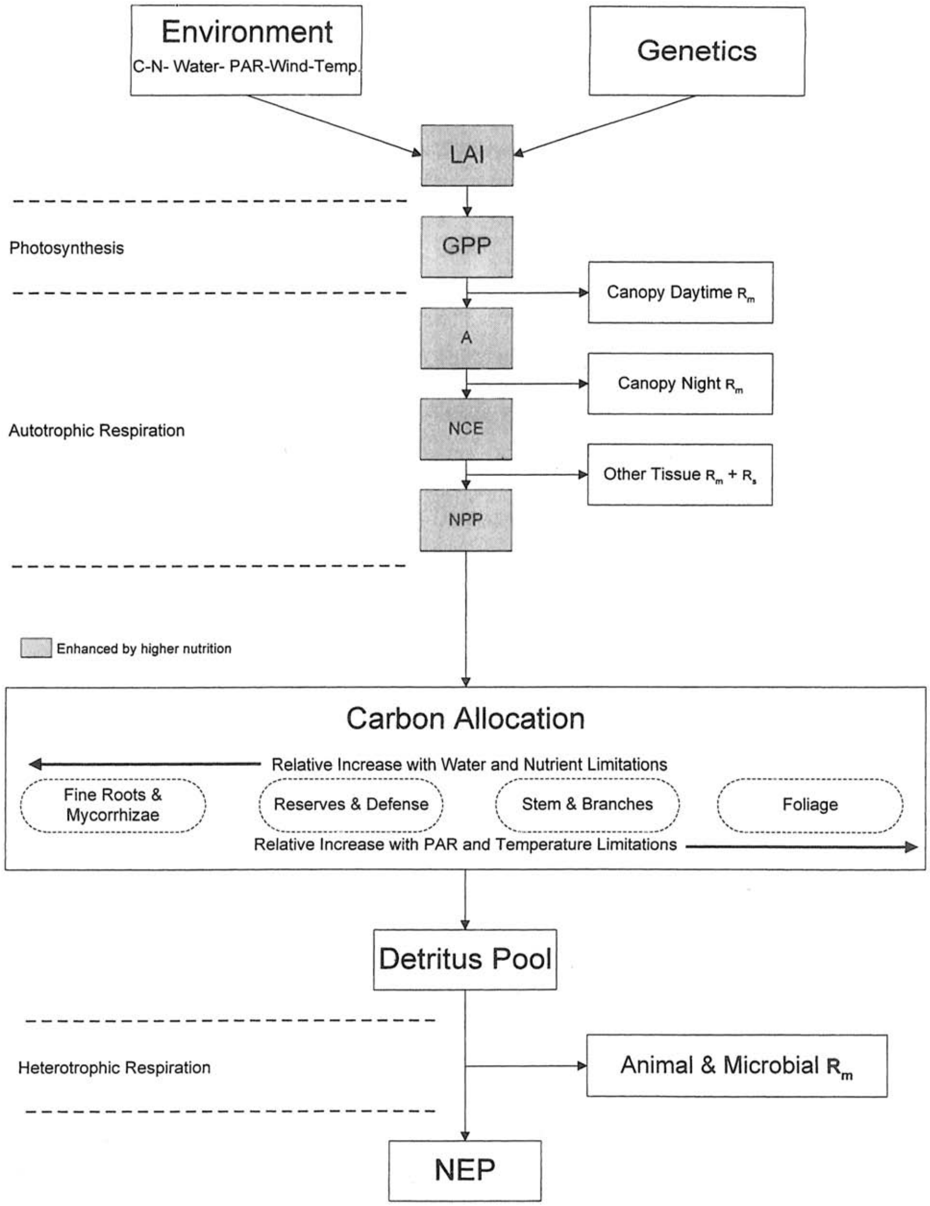

FIGURE 3.1. Carbon balance models that are coupled to water and nutrient cycling operate by predicting carbon uptake and losses through a series of processes, starting with photosynthesis and the absorption of solar radiation by leaves. Gross primary production (GPP) is further limited by other environmental variables affecting canopy stomatal conductance. Deducting foliar maintenance respiration during the daylight hours provides an estimate of net assimilation (A). Including canopy respiration at night yields an estimate of daily net canopy exchange (NCE) for a 24-hr period. Net primary production (NPP) is calculated by accounting for additional autotrophic losses associated with synthesis (R_s) and maintenance (R_m) throughout each day. NPP is partitioned into various components based on schemes associated with C:N ratios which change with the availability of water and nutrients. Leaf and fine-root turnover are the major contributors to litter on a seasonal basis, but all biomass components eventually enter the detrital pool. The annual turnover of leaves and roots is correlated with seasonal variation in LAI, specific leaf area, and nitrogen content. Decomposition of litter and release of CO_2 by heterotrophic organisms are functions of substrate quality (C:N ratio), temperature, and moisture conditions. Net ecosystem production (NEP) is calculated as the residual, after deducting heterotrophic respiration (R_h).

in most ecosystems because it remains unoxidized for centuries. It is the most important long-term carbon storage site in ecosystems. We delay discussion on soil humus until Chapter 4.

Figure 3.1 provides a general framework for modeling carbon flow through ecosystems and is the basis for organizing the material presented in this chapter. All of the environmental variables associated with modeling the water cycle (Chapter 2) are closely linked with the carbon cycle. Atmospheric carbon dioxide concentrations and the availability of soil nitrogen (N) must also be considered when modeling photosynthesis, carbon allocation, and respiration. Confidence in the reliability of models has greatly increased with the development of an eddy correlation technique that uses fast-response sensors to record the net exchange of CO_2 and water vapor from forests and other types of terrestrial ecosystems.

As ecosystem scientists, we consider the exchange of carbon into the system through photosynthesis to be a positive flux and respiration to represent a loss to the atmosphere. Atmospheric scientists would consider the signs to be reversed. Net ecosystem exchange (NEE) measured during the daylight hours includes gross photosynthesis (P_g or GPP), photorespiration (R_p), maintenance respiration (R_m), and synthesis (growth) respiration (R_s) of autotrophic plants, as well as heterotrophic respiration (R_h) by animals and microbes:

$$\text{Day NEE} = P_g - R_p - R_m - R_S - R_h. \tag{3.1}$$

At night the photosynthetic terms, P_g and R_p, are absent:

$$\text{Night NEE} = -R_m - R_s - R_h = -R_e \tag{3.2}$$

where R_e is total ecosystem respiration, exclusive of R_p. On a given day, R_e is largely controlled by temperature, which allows us to make adjustments for its rise during daylight periods from values recorded at lower temperatures during the night. Gross ecosystem production (GEP) includes photorespiration, which is usually small, so GEP is often assumed to approximate P_g:

$$\text{GEP} = \text{Day NEE} + \text{Day } R_e = P_g - R_p \approx \text{GPP}. \tag{3.3}$$

To separate the sources of respired CO_2, a series of chambers are often installed and CO_2 effluxes monitored at frequent intervals from soil, stem, branches, and leaves. Alternatively, respiration sources can be identified by monitoring the isotopic composition of carbon ($\delta^{13}C$) and oxygen ($\delta^{18}O$) in CO_2 diffusing into the turbulent transfer steam. The scientific value of full system analyses with eddy correlation techniques has proved immense, particularly when conducted over a series of years (Goulden *et al.,* 1996). Eddy-flux installations therefore serve for testing the underlying assumptions and accuracy of stand-level ecosystem models.

Among species (and genetic varieties), important differences exist in the pattern of carbon allocation. These differences affect competitive relationships (Chapter 5), the susceptibility of trees and other plants to various stresses (Chapter 6), as well as the annual carbon balance of a stand. Foresters have developed good empirical models to predict volume growth of trees and whole stands. These are helpful in supporting general assumptions built into stand-level ecosystem models; stem growth, however, is highly dependent on the fraction of NPP allocated to foliage versus roots, and so is difficult to predict as environmental conditions change seasonally and from site to site. Different theories that provide a basis for modeling carbon allocation are presented in this chapter. We will identify general principles governing the way the environment affects carbon allocation seasonally and over the course of a year, and apply these principles in later chapters.

II. PHOTOSYNTHESIS

Photosynthesis is the process by which plants convert atmospheric CO_2 to carbon products. Photosynthesis takes place within cells containing chloroplasts. Chloroplasts contain chlorophyll and other pigments that absorb sunlight. Energy from the sun causes electrons to become excited and water molecules to be split into hydrogen and oxygen:

$$CO_2 + 2H_2O + \text{light energy} \rightarrow CO_2 + 4H^+ + O_2 \rightarrow CH_2O + H_2O + O_2. \qquad (3.4)$$

The hydrogen joins with carbon from CO_2 to produce simple three- or four-carbon products which ultimately are synthesized into larger molecules that are incorporated into biomass or consumed in metabolic processes. Photosynthesis is restricted by both physical and biochemical processes and involves some reactions that require light and others that can take place in the dark. At the leaf surface, stomata limit the diffusion of carbon dioxide into intercellular spaces. Inside leaves, CO_2 must dissolve in water and pass through cell walls to reach the sites where chemical reactions take place within chloroplasts.

Net photosynthesis has three separate, potentially limiting components: (a) light reactions, in which radiant energy is absorbed and used to generate high-energy compounds (ATP and NADPH); (b) dark reactions, which include the biochemical reduction of CO_2 to sugars using the high-energy compounds previously generated; and (c) the rate at which CO_2 in ambient air is supplied to the site of reduction in the chloroplast.

In the light reactions, radiation absorbed by chlorophyll causes excitation of electrons which are transferred down a chain of specialized pigment molecules to reaction centers where high-energy compounds are formed, water is split, and O_2 released [Eq. (3.4)]. The initial part of the light reaction is only limited by the irradiance and amount of chlorophyll present. The rate of electron transfer is sensitive to temperature but independent of CO_2 concentrations. In the dark reactions, C_3 plants use the enzyme ribulose-bisphosphate carboxylase–oxygenase (Rubisco) for the primary fixation of CO_2. In light, photorespiration also occurs in the process of generating the substrate ribulose bisphosphate (RuBP), particularly when the ratio of O_2 to CO_2 increases within the chloroplast. Additional high-energy compounds are required to create six-carbon sugars, and, as a result, additional CO_2 is respired. Dark reactions are CO_2 and temperature limited, and also dependent on sufficient nitrogen and other substrate being available to synthesize the Rubisco enzyme. The rate at which CO_2 can be supplied to chloroplasts is limited by the CO_2 partial pressure and by stomatal conductance, which limits diffusion of CO_2 to 0.625 times that of water vapor, because of the difference in molecular mass.

Farquhar *et al.* (1980) developed a set of basic equations that incorporate the limiting processes to net assimilation of CO_2. Specifically, the equations consider limitations by enzymes (A_v), by electron transport (A_j), and by stomatal conductance (g_{CO_2}). Enzyme-limited assimilation (A_v) is defined as

$$A_v = [V_{max}(c_i - G^*)/[K_c(1 + pO_2/K_0) + c_i]] - R_c. \tag{3.5}$$

where V_{max} is the maximum carboxylation rate when the enzyme is saturated, pO_2 is the ambient partial pressure of oxygen, K_c and K_0 are Michaelis–Menten constants for carboxylation and oxygenation by Rubisco, respectively; c_i is the partial pressure of CO_2 in the chloroplast, G^* is the CO_2 compensation partial pressure in the absence of dark respiration, and R_c is the dark respiration by the leaf. K_c, K_0, and V_{max} are temperature sensitive and are adjusted from a base rate at 25°C (298.2 K) with Arrhenius-type relationships (with K_x representing all three variables):

$$K_x = K_{x,25} \exp[(E_x/298.2R)(1 - 298.2/T_c)] \tag{3.6}$$

where T_c is the canopy temperature (K), R is the universal gas constant (8.314 J mol^{-1} K^{-1}), and E_x refer to the approximate activation energies for K_c, K_o, and V_{max}.

When electron transport limits photosynthesis (A_j):

$$A_j = (J/4)[(c_i - G^*)/(c_i + 2G^*)] - R_c \tag{3.7}$$

where J is the potential rate of electron transport, which is related to the maximum light-saturated rate of electron transport and the absorbed irradiance. The sensitivities of A_j and R_c to temperature are also considered in equations similar to Eq. (3.6).

Finally, after accounting for effects of PAR and temperature on photosynthesis, stomatal conductance to CO_2 (g_{CO_2}) is calculated, assuming that c_i (partial pressure of CO_2 within the chloroplasts) is proportional to ambient CO_2 partial pressure (c_a):

$$c_i = c_a - (A/g_{CO_2}) \tag{3.8}$$

A semiempirical model developed by Ball *et al.* (1987) described stomatal conductance for CO_2 diffusion (g_{CO_2}) as:

$$g_{CO_2} = g_0 + (g_1 A h P)/(c_a - G) \tag{3.9}$$

where g_0 is the minimum stomatal conductance and g_1 is an empirical coefficient which represents the composite sensitivity of conductance to assimilation, CO_2, humidity, and temperature, h is the relative humidity at the leaf surface, P is the atmospheric pressure, G is the CO_2 compensation point, and c_a is the ambient partial pressure of CO_2 at the leaf surface. Equation (3.9) has been modified to express relative humidity as vapor pressure deficit with reference to leaf temperature (Leuning, 1995). Dewar (1995) suggested a more mechanistic form of the equation which reflects stomatal guard cell response and has the potential to incorporate restrictions on water uptake that affect stomatal conductance (Chapter 2).

Many additional equations are required to solve all the unknowns in such fundamental models, but Eqs. (3.5) to (3.9) include all the major variables. They allow prediction of the consequence of rising levels of CO_2 in the atmosphere, while also identifying potential limitations associated with the availability of nitrogen, light, temperature, and all the additional variables affecting stomatal conductance discussed in Chapter 2. This basic model has been applied in temperate deciduous (Baldocchi and Harley, 1995), temperate evergreen (Thornley and Cannell, 1996), tropical (Lloyd *et al.,* 1995), Mediterranean (Valentini *et al.,* 1991), and a variety of boreal forests (Wang and Polglase, 1995) and will serve as a reference against which we will compare more empirical models. For a critical review of the basic equations and modeling assumptions, see Leuning *et al.* (1995).

Because of the interactions of light, CO_2, and the rate at which RuBP can be regenerated, net photosynthesis always shows an asymptotic curve with increasing irradiance (Fig. 3.2). With reference to photosynthesis, where light energy in different wavelengths is involved, irradiance is expressed in units of moles (mol) per photon of light, where 1 mol is equivalent to the atomic mass of carbon (12) or molecular mass of CO_2 (44) fixed and 4.6 μmol photons $m^{-2} s^{-1} = 1 J m^{-2} s^{-1}$ or $1 W m^{-2}$ of absorbed PAR (APAR). Below some minimum irradiance level, net carbon uptake (assimilation, A) is negative in reference to the leaf, as foliar respiration exceeds photosynthesis. As irradiance increases, a compensation point is reached where the uptake of CO_2 through photosynthesis is exactly balanced by losses through respiration. Above the *light compensation point,* uptake increases linearly until the availability of RuBP or CO_2 limits the process. Increasing ambient CO_2 increases the maximum net photosynthetic rates (A_{max}) but not the linear part of the curve, because at low irradiance photochemistry, not CO_2, limits the process.

The apparent quantum efficiency (α) is the slope (A/PAR) of the linear part of the photosynthesis–irradiance curve, that is, the rate of increase in assimilation with irradiance at levels below those at which CO_2 has an effect (e.g., no photorespiration occurs). The apparent quantum efficiency is relatively conservative, with an average of ~0.03 mol CO_2/mol photons of APAR (equivalent to 1.65 g C MJ^{-1} PAR absorbed) throughout most forest canopies (and far below the theoretical maximum of 0.08 mol CO_2/mol photons of APAR), but it changes, as one might expect, as chlorophyll levels fluctuate (Jones, 1992; Waring *et al.,* 1995a).

The maximum rate of assimilation, on the other hand, decreases from the top to the bottom of a forest canopy (Fig. 3.3a). A_{max} is generally higher in the leaves of deciduous tree species than in evergreens (Ceulemans and Saugier, 1991), and the longer that leaves live, the more their A_{max} is reduced (Reich *et al.,* 1995a). One of the underlying reasons for these relationships is that thicker leaves associated with evergreens offer a more restricted diffusion pathway to CO_2 than deciduous leaves (Robinson, 1994). A second reason is that evergreen foliage tends to hold less nitrogen per unit area than deciduous leaves (Field and Mooney, 1986; Ellsworth and Reich, 1993; Reich and Walters, 1994). Because some of the nitrogen in leaves is in forms other than photosynthetic structures, total nitrogen content is not always directly related to photosynthetic capacity. Kull and Jarvis (1995) showed theoretically how measurements made on foliage collected from the upper part of a canopy might allow prediction of the amount of nitrogen bound in photosynthetic machinery throughout the entire canopy. Field investigations in boreal forests, however, do not fully support this interpretation (Dang *et al.,* 1997).

Both canopy leaf nitrogen and canopy leaf mass tend to increase with absorbed PAR (Kull and Jarvis, 1995). Because highly illuminated foliage contains more cell layers than shaded leaves, *specific leaf mass* (SLM, kg m^{-2}) and A_{max} generally decrease in parallel

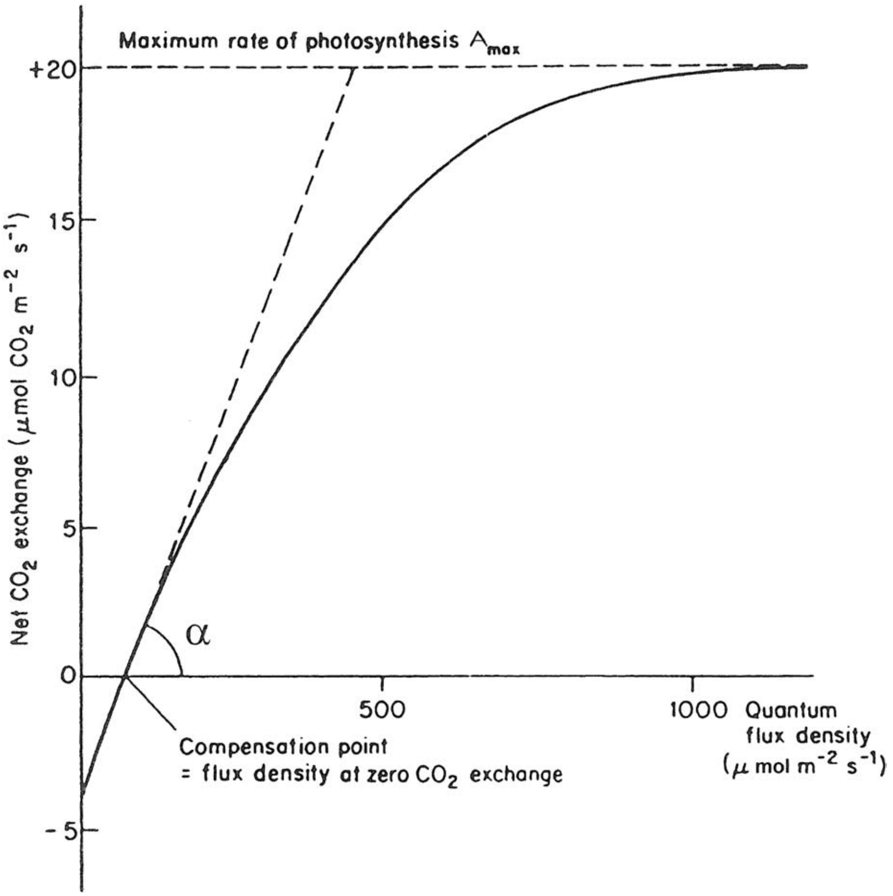

FIGURE 3.2. Representative net photosynthetic response (A) to increasing irradiance. The slope (α) at low irradiances, denoted by the dotted line, represents the apparent quantum efficiency. Light compensation occurs where net CO_2 exchange is zero, and gross photosynthesis equals dark respiration. Net photosynthesis continues to increase asymptotically with irradiance until maximum rates (A_{max}) are achieved.

through a canopy (Fig. 3.3b). Specific leaf mass, or its reciprocal specific leaf area ($m^2 kg^{-1}$), is an essential component of allocation models, and it tends to change in predictable ways not only with the light environment, but also with the availability of nitrogen and general harshness of the environment (Specht and Specht, 1989; Pierce *et al.,* 1994). The actual concentration of chlorophyll pigments per unit of leaf surface area, however, offers a more accurate measure of quantum efficiency and photosynthetic capacity than total nitrogen or specific leaf mass (Waring *et al.,* 1995a). The amount of chlorophyll per square meter of foliage varies considerably among tree species and with season (Escarré *et al.,* 1984). When expressed as chlorophyll per unit of ground surface area, which integrates the entire canopy, values may be quite similar for evergreen and deciduous forests (Cannell, 1989; Reich *et al.,* 1995b; Dang *et al.,* 1997).

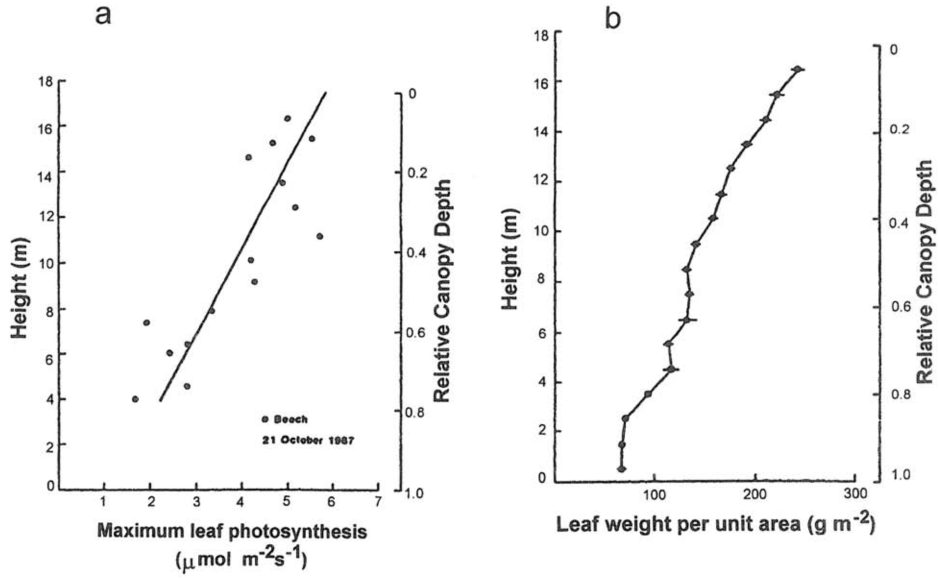

FIGURE 3.3. (a) Photosynthetic capacity (A_{max}) decreased through a *Nothofagus* canopy in parallel with changes in leaf weight per unit area. (b) Leaf weight per unit area in a pure stand of *Nothofagus* growing in New Zealand decreased from the top to the bottom of the canopy as a function of light intercepted. (From Hollinger, 1989.)

The optimum temperature range for photosynthesis varies with species but is commonly between 15° and 25°C for temperate trees, with extremes reported between about 10° and 35°C (Kozlowski and Keller, 1966; Mooney, 1972). Tropical trees show higher optimum temperatures, between 30° and 35°C (Lloyd *et al.,* 1995). A shift in temperature optimum may occur if other factors change the intercellular level of CO_2 or the efficiency of the photosynthetic machinery. In general, increased internal CO_2 concentrations allow the temperature optimum to be shifted upward by reducing photorespiration. At temperatures above 40°C, gross photosynthesis decreases abruptly because of changes in chloroplast and enzyme activity (Berry and Downton, 1982). Protein denatures at 55°C (Levitt, 1980). As a result of these factors, the net carbon uptake by leaves usually increases gradually to an optimum temperature and then decreases more abruptly as the maximum temperature limit is approached. The broadness of the temperature optimum, together with its ability to shift with season (Strain *et al.,* 1976; Slatyer and Morrow, 1977), reduces its significance for modeling gross photosynthesis, except perhaps where species may have become geographically isolated and survive, if not thrive, under a changed climate from that for which they originally evolved (Waring and Winner, 1996).

Because trees are often adapted to a wide range of seasonal temperature variations, the frequency and duration of extremes are more critical than mean temperature in limiting photosynthesis (Van *et al.,* 1994; Perkins and Adams, 1995). For example, a 3-hr exposure of seedlings of *Pinus sylvestris* to temperatures between −5° and −12°C reduced quantum efficiency from 10 to over 80% (Strand and Öquist, 1985). Recovery may be delayed for weeks or months with repeated exposure to frost, particularly if leaves are exposed to high irradiance (Strand and Öquist, 1985). Different mechanisms may operate, but increased respiration that follows exposure to low temperatures suggests that repair of damaged membranes is involved (see review by Hällgren *et al.,* 1991). Short exposure to high temperatures likewise may be injurious and may alter competitive relationships among species (Bassow *et al.,* 1994).

Water is essential to all living cells, so any reduction in its availability might be expected to affect photosynthesis as well as many other processes. In Chapter 2, we discussed the water relations of forests. Here, only the effects of water limitations on photosynthesis and the related process of photorespiration will be covered. The availability of water in leaf tissue is not directly dependent on the water content. Changes in cell wall elasticity, in membrane permeability, and in concentration of solutes in cells counterbalance the effects of decreasing water content (Edwards and Dixon, 1995). Diurnal variations of 5–10% in leaf water content relative to saturation often have no direct effect on photosynthesis (Hanson and Hitz, 1982). Eventually, if leaf tissue continues to lose water, stomata are forced to close, and the rate of CO_2 diffusion into the leaf is reduced or halted. Under extended drought, some of the Rubisco enzyme will be broken down, reducing the biochemical capacity of the photosynthetic system. Concentrations of chlorophyll and other pigments important in photochemical reactions are also reduced (Farquhar and Sharkey, 1982; Jones, 1992). The main effects of water limitations on photosynthesis are through reduction in stomatal conductance, as described in Chapter 2.

III. AUTOTROPHIC RESPIRATION

Autotrophic respiration (R_a) involves the oxidation of organic substances to CO_2 and water, with the production of ATP and reducing power (NADPH):

$$O_2 + CH_2O \rightarrow CO_2 + H_2O. \tag{3.10}$$

Total autotrophic respiration consists of two major components associated with the metabolic energy expended in the synthesis of new tissue and in the maintenance of living tissue already synthesized.

A. Maintenance Respiration

Maintenance respiration, the basal rate of metabolism, includes the energy expended on ion uptake and transfer within plants. Repair of injured tissue may greatly increase the basal rates of metabolism. Because trees accumulate a large amount of conducting and storage tissues as they age, the observed decrease in relative growth rate associated with age has often been assumed to reflect increasing maintenance costs (Whittaker, 1975; Waring and Schlesinger, 1985). Most of the conducting tissue in trees, however, is sapwood, which contains relatively few living cells (Fig. 3.4; Table 3.1). Enzymatic activity, associated with N concentration in living tissue, is also much lower in the sapwood than in leaves (Amthor, 1984; Ryan, 1991a, 1995). Leaf tissue, with 2% N, might respire about 0.45% of their weight daily at 10°C and 0.9% at 20°C. In comparison, an equal weight of sapwood metabolizes at less than one-tenth that of foliage. As a result, the annual

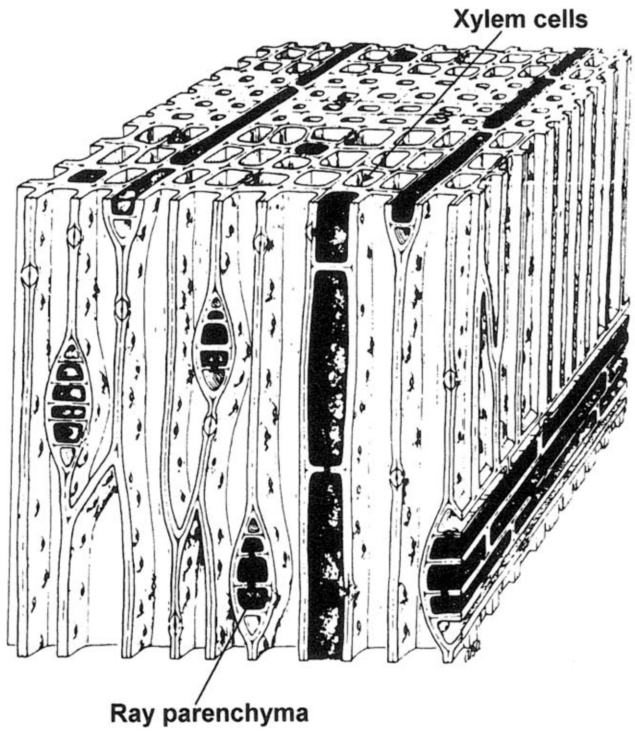

FIGURE 3.4. Most of the cells in the sapwood of trees are dead, which permits efficient transport of water. Traversing the wood, however, are bands of living parenchyma cells (darkened) which store carbohydrates. Diagram shows a redwood (*Sequoia sempervirens*). (From Weier *et al.,* 1974, by copyright permission of John Wiley & Sons, Inc.)

maintenance cost of sapwood in large trees is generally less than 10% of annual GPP (Fig. 3.5).

In modeling maintenance respiration (R_m), an exponential increase with temperature is normally observed within the range of biological activity, as described by the formula

$$R_m(T) = R_0 Q_{10}^{[(T-T_0)/10]} \tag{3.11}$$

where R_0 is the basal respiration rate at $T_0 = 0°C$ (or other reference temperature). The parameter Q_{10} is the *respiration quotient* and represents the change in the rate of respiration for a 10°C change in temperature (T). The Q_{10} is relatively conservative, usually between about 2.0 and 2.3. Under field conditions, where daily temperature variation is large, the nonlinearity in the response of maintenance respiration should be taken into account. This has been accomplished by fitting a sine function to minimum–maximum temperature differences and integrating the response not only daily, but throughout the year (Hagihara and Hozumi, 1991; Ryan, 1991a). As mentioned previously, R_0 is highly variable, depending on the protein (or N) content in the tissue (Jarvis and Leverenz, 1983). Seasonal changes in LAI and fine-root mass, together with possible variation in the ratio of active to inactive enzymes, make it difficult to estimate carbon expenditures annually

TABLE 3.1

Percentage of Living Parenchyma Cells in the Sapwood of Representative Hardwoods and Conifers Native to the United States[a]

Species	%	Range
Hardwoods		
Populus tremuloides	9.6	4.4
Betula alleghaniensis	10.7	0.9
Fagus grandifolia	20.4	5.3
Quercus alba	27.9	—
Liriodendron tulipifera	14.2	2.5
Robinia pseudoacacia	20.9	3.1
Acer saccharum	17.9	5.2
Tilia americana	6.0	3.8
Conifers		
Pinus taeda	7.6	1.6
Larix occidentalis	10.0	1.1
Picea engelmannii	5.9	2.5
Pseudotsuga menziesii	7.3	2.1
Tsuga canadensis	5.9	0.7
Abies balsamea	5.6	2.3
Sequoia sempervirens	7.8	2.5
Taxodium distichum	6.6	2.6

[a]After Panshin *et al.* (1964).

to much better than ±25%, but this is a great improvement over earlier efforts and provides an important advance in constructing tree and stand carbon balances (Ryan, 1991b, 1996b).

Some special concerns should be mentioned in relation to measuring respiration with chambers. When chambers are placed over thin bark surfaces that have photosynthetic capacity, the respiration measured may overestimate (by up to 100%) the net exchange from such surfaces (Linder and Troeng, 1981). Also, when determining root respiration, care must be taken because maintenance respiration is reduced exponentially as CO_2 concentrations increase; thus, rates in the soil, where CO_2 concentrations may exceed 5000 ppm, are only one-tenth of those recorded at atmospheric concentrations (Qi *et al.,* 1994; Burton *et al.,* 1997).

B. Growth and Synthesis Respiration

Growth requires the metabolism of more resources than can be found in the final product. Rates of *synthesis respiration* (R_s) for various tissues differ, depending on the biochemical pathways involved. The production of 1 g of lipid would require 3.02 g of glucose, whereas 1 g of lignin, protein, or sugar polymer might require, respectively, 1.90, 2.35, and 1.18 g of glucose (Penning de Vries, 1975). More recently, empirical relations have been derived to estimate the total cost of construction based on correlations with the heat of combustion, ash, and organic N content of tissue and the biochemical constituents (McDermitt and

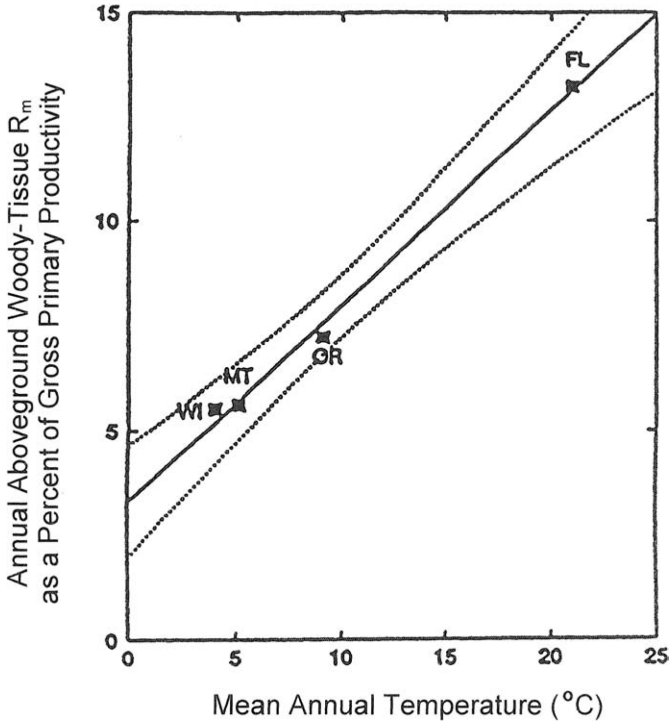

FIGURE 3.5. Maintenance respiration of aboveground woody tissue in evergreen trees growing in Wisconsin (WI), Montana (MT), Oregon (OR), and Florida (FL) was usually <10% of estimated gross primary production (GPP) but increased linearly with mean annual temperature ($y = 2.76 + 0.48x$, $r^2 = 0.99$). (From *Oecologia,* "Stem maintenance respiration of four conifers in contrasting climates," M. G. Ryan, S. T. Gower, R. M. Hubbard, R. H. Waring, H. L. Gholz, W. P. Cropper, and S. W. Running, Volume 101, p. 138, Fig. 4, 1995, © 1995 by Springer-Verlag.)

Loomis, 1981; Vertregt and Penning de Vries, 1987; Williams *et al.,* 1987; Griffin, 1994). In Table 3.2, the cost of producing various tissues and organs, based on their biochemical composition, is presented. The total construction cost for a gram of pine shoot is equivalent to 1.57 g glucose (Chung and Barnes, 1977). Assuming foliage is 50% C, 1.28 g C in glucose would produce 1 g C in foliage. For large trees, synthesis costs are usually assumed to be about 25% of the carbon incorporated into new tissues (Ryan, 1991a,b). For smaller trees, particularly deciduous species with high concentrations of proteins in foliage and other organs, synthesis costs may rise to 35% of the carbon sequestered in biomass.

To assess the contribution of synthesis respiration to total plant respiration, monitoring must include periods in both active and dormant seasons. Periods of rapid growth can be monitored by recording the expansion in diameter of calibrated bands placed around branches, stems, and large-diameter roots, and through measuring stem elongation (Dougherty *et al.,* 1994). Dormancy and annual growth increments should be confirmed by anatomical inspection (Gregory, 1971; Emmingham, 1977) so that respiration rates measured throughout the growing season can be properly interpreted (Ryan *et al.,* 1995).

TABLE 3.2.
Estimated Construction Costs of Various Organs and Tissues[a]

Type of tree	Organ or tissue	Total construction cost (g C required/g C in product)
Pine	Needles	1.28
	Branches	1.21
	Bark	1.30
	Roots	1.20
Eucalyptus	Phloem	1.18
	Cambium	1.05
	Sapwood	1.11
	Heartwood	1.14

[a]After Chung and Barnes (1977). Glucose equivalents were converted by recognizing that glucose is 40% C and by assuming that the dry weight of all products contained 50% C.

The determination of root growth and maintenance is particularly difficult because of the heterogeneity of roots in size, distribution, and degree of colonization with symbiotic organisms (mycorrhizal fungi and nitrogen-fixing bacteria). In most field programs where attempts are made to separate the sources of respiration, chambers or CO_2 traps are placed over the litter surface and an estimate of total CO_2 efflux is obtained. When such data are available throughout the year, they provide some constraints on the estimate of belowground carbon allocation to roots and the contribution of heterotrophic respiration.

Raich and Nadelhoffer (1989) provided an indirect approach to estimate belowground carbon allocation by assuming that, over a year, leaf litter and root turnover would add an amount of carbon approximately equal to that respired from the soil, and that there would be no net change in the soil carbon pool. Under these conditions, soil respiration minus leaf litterfall approximately equals root production plus root respiration. With soil respiration and litterfall data assembled from a range of forests from boreal to tropical, Raich and Nadelhoffer presented a linear relationship between carbon in leaf litterfall and the total carbon allocation to small-diameter roots (Fig. 3.6). Ryan *et al.* (1996b) extended the approach to ecosystems with a significant annual increment of coarse roots by assuming that total belowground carbon allocation was equal to the difference between annual soil respiration and aboveground litterfall plus coarse root increment. The carbon allocated to NPP_{roots} is often assumed to be about half the total. The general application of this approach requires a measurement of annual litterfall or knowledge of the fraction of the total foliage mass that turns over annually, taking into account a loss of mass (usually 10–25%) per unit area before leaves are shed (Chapter 4).

IV. HETEROTROPHIC RESPIRATION

The detritus produced by autotrophic plants serves as food or substrate for heterotrophic organisms which respire CO_2 or methane (CH_4). In estimating carbon balances of ecosystems, the rate that litter (including large woody components) decomposes (above- and belowground) is important to quantify. In Chapter 4, we discuss how the activities of micro- and macroorganisms respond to changes in the size, biochemical composition, and

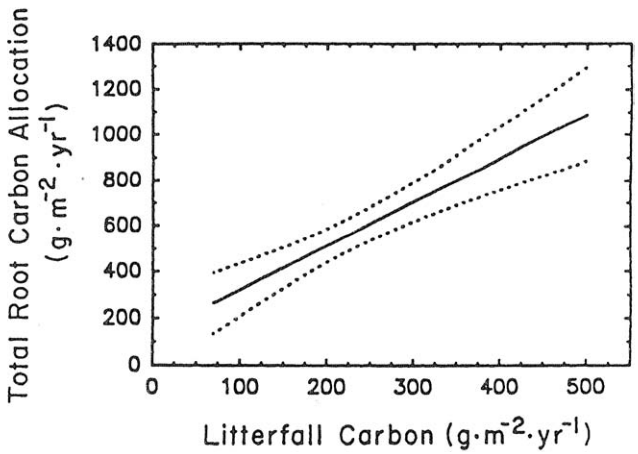

FIGURE 3.6. Predicted rates of total belowground carbon allocation in forest ecosystems are linearly related to aboveground litterfall ($y = 130 + 1.92x$, $r^2 = 0.52$). Belowground carbon allocation was calculated as the difference between soil respiration and litterfall for individual forests where the soil carbon pool was assumed to be in approximate steady state over a year. (From Raich and Nadelhoffer, 1989.)

physical environment associated with different substrates, with the goal of estimating CO_2 evolution from the breakdown and decomposition of all forms of detritus. In this section, we focus on leaf and fine-root detritus because these components turn over rapidly and are therefore likely to contribute the most to seasonal fluctuations in heterotrophic respiration.

When heterotrophic respiration is monitored by enclosing samples of fresh leaf or fine-root litter within small-mesh nylon bags, the mass loss per unit time can be measured, and, because organic matter is approximately 50% carbon, the CO_2 evolved can be calculated. Alternatively, under laboratory conditions, litter samples may be placed in chambers with controls on moisture and temperature and CO_2 efflux directly monitored. From a combination of studies, three major variables have been identified as limiting heterotrophic respiration: substrate quality, relative water content, and temperature.

A. Substrate Quality

Substrate quality is correlated with the energy that microorganisms must expend in processing detritus. Sugars, starch, fats, and proteins are relatively reduced forms of carbon and easily metabolized, whereas tannins, cellulose, and lignin are more oxidized forms and less efficiently metabolized. A crude index of substrate quality is its nitrogen content per gram C, usually expressed as a C:N ratio, with high ratios indicative of material that will be processed very slowly. Conifer wood at 0.1% N has a C:N ratio of 500:1, whereas fresh hardwood leaves with 2% N have a C:N ratio of 25:1. Over time, C:N ratios in decomposing substrates are reduced as microbes process the carbon, and nitrogen accumulates in their biomass. Microbial biomass has a C:N range from about 4 to over 20, with bacteria having <10 and fungi >10 (Sparling and Williams, 1986; Schimel *et al.,* 1989; Martikainen and Palojarvi, 1990; Lavelle *et al.,* 1993). Fungi have some advantage over bacteria in forest ecosystems because of their higher C : N ratios. Unless environmental conditions become unfavorable and cause microbes to die, little nitrogen will be released from the substrate until its C : N ratio is reduced to below that of the organisms involved. In reality, the simple C : N ratio is not a very precise index; a better index is derived from the ratio of lignin to nitrogen (Melillo *et al.,* 1982), or other biochemical constituents which reflect the free energy extractable from a given mass of substrate.

B. Moisture and Temperature

The metabolic activity of microorganisms also varies with moisture and temperature of surface litter and soil. In surface litter, fairly stable metabolic activity is usually observed until the substrate is nearly dry (Fig. 3.7). In soils, however, microbial activity appears to be reduced more linearly with decreasing gravimetric water content and to show a log–linear decrease with falling Ψ_{soil} (Orchard *et al.,* 1992). The temperature response is usually exponential but highly variable. Note in Fig. 3.7 that over the range from 4° to 35°C that the Q_{10} for microbial activity on jarrah leaf litter is 1.6 whereas the Q_{10} on karri substrate is 2.3. The base reference temperature also varies depending on the climate in which specific microorganisms have evolved. In general, decomposition rates are extremely low below 0°C, increase rapidly between 10° and 30°C, and decrease at temperatures >40°C (Ågren *et al.,* 1991). These nonlinear responses to moisture and temperature provide, together with lignin content or related indices of substrate quality, the foundation for modeling heterotrophic respiration and decomposition in forest and other terrestrial ecosystems (Jansson and Berg, 1985; O'Connell, 1990; Ågren *et al.,* 1991).

C. Determining the Sources of Respired CO_2 from Stable Isotope Analyses

The isotopic composition of carbon and oxygen in CO_2 differs significantly, depending on whether it is derived from leaves, stems, roots, or decaying organic matter. This allows us to discriminate the relative contribution of different sources of CO_2 in soil, air, and leaves of forest canopies (Keeling, 1958; Sternberg, 1989; Flanagan *et al.,* 1997a). In the biochemical synthesis of various plant constituents from sugars, some isotopic fractionation occurs. For example, lignin is depleted in ^{13}C compared to whole cellulose (Benner *et al.,* 1987). It is also likely that some isotopic fractionation occurs during microbial respiration, leading to a ^{13}C enrichment in microbial carbon compared to plant-derived carbon in soils (Macko and Estep, 1984).

During the process of photosynthesis, a portion of the CO_2 that enters the leaf and equilibrates with chloroplast water is not fixed and diffuses back out of the leaf with an altered oxygen isotopic ratio. The oxygen in CO_2 evolved from the soil has exchanged with soil water and isotopically matches that source. The isotopic composition of water in the xylem does not change from that in the soil, until transpiration from the leaf takes place. During transpiration, ^{18}O is discriminated against, so that leaf water is enriched and the vapor released into the atmosphere is depleted. The CO_2 metabolically respired by plants is also depleted in ^{13}C compared to the atmosphere because, during photosynthesis,

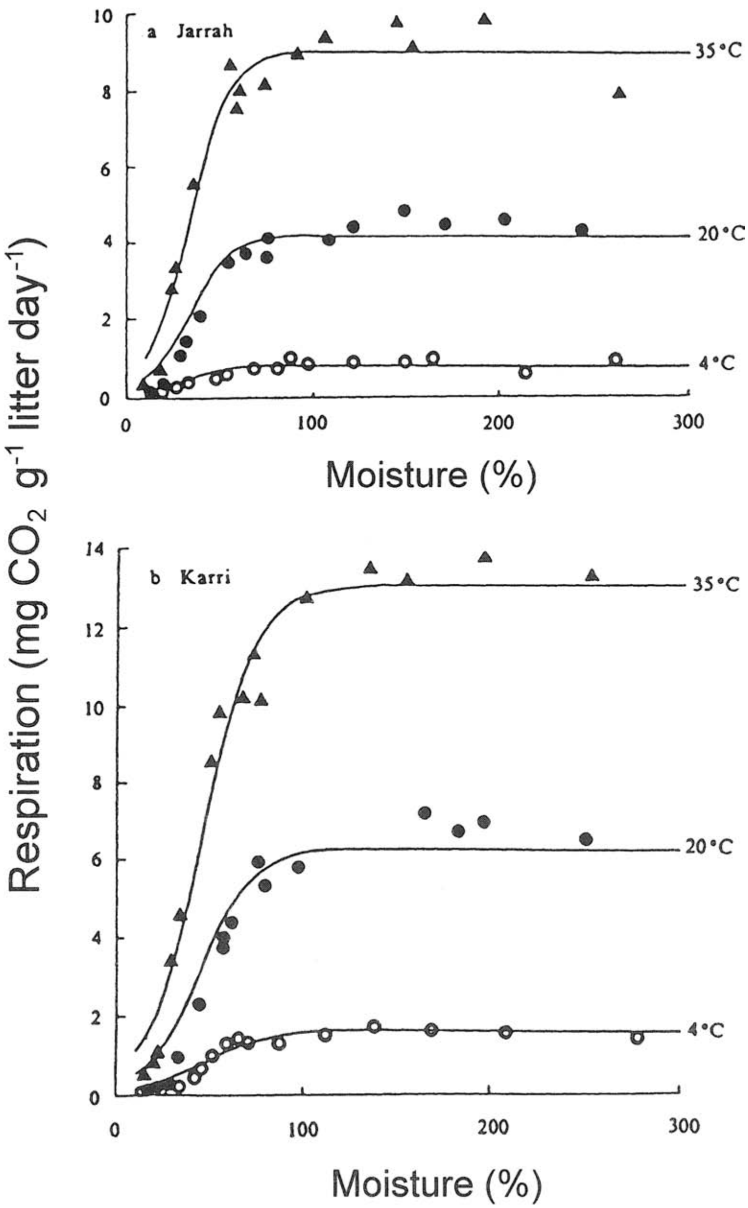

FIGURE 3.7. Laboratory incubation of foliage from (a) jarrah (*Eucalyptus marginata*) and (b) karri (*Eucalyptus diversicolor*) show that microbial respiration (R_h) increases exponentially with temperature between 4° and 35°C, and is relatively insensitive to changes in litter moisture content until below about 100% or near saturation (not shown). Jarrah litter represents a less favorable substrate for decomposition than that of karri. Separate equations for the two species that combined both temperature and moisture responses accounted for 93 to 94% of the observed variation in measured respiration. (Reprinted from *Soil Biology and Biochemistry,* Volume 22, A. M. O'Connell, "Microbial decomposition (respiration) of litter in eucalypt forests of southwestern Australia: An empirical model based on laboratory incubations," pp. 153–160, Copyright 1990, with kind permission of Elsevier Science Ltd, The Boulevard, Langford Lane, Kidlington OX5 1GB, UK.)

^{13}C is discriminated against during diffusion through stomata and also by Rubisco. As a result of these differences in isotopic fractionation, which are now well established and can be quantitatively modeled, it has become possible to separate the major sources of CO_2 evolved diurnally and seasonally from forest ecosystems (Buchmann *et al.,* 1997; Flanagan *et al.,* 1997a,b).

Sternberg (1989) developed a two-ended gas-mixing model to describe the relationship between the concentration and isotope ratio of CO_2 within a forest canopy. He assumed that four different fluxes influence the forest atmosphere: photosynthetic CO_2 uptake (F_p), turbulent flux of CO_2 out of the forest (F_a), respiration (F_r), and turbulent flux of CO_2 into the forest (F_{fa}). The relationship is described by

$$\delta_f = ([CO_2]_a/[CO_2]_f)(\delta_a - \delta_r)(1 - P) + \delta_r + P\Delta_a \tag{3.12}$$

where $[CO_2]$ is the concentration of CO_2 and δ is the stable isotope ratio of CO_2; the subscripts a and f represent bulk atmosphere and forest, respectively; P is the uptake of carbon dioxide by photosynthesis relative to the total loss of CO_2 from the forest $[P = F_p/(F_p + F_{fa})]$; δ_r is the isotopic ratio of CO_2 respired by plants and soil; and Δ_a is the isotopic discrimination that occurs during photosynthetic gas exchange.

Under conditions where removal of carbon dioxide from the forest by photosynthesis is small relative to turbulent mixing, P tends toward zero and Eq. (3.12) is reduced, as presented by Keeling (1958), to

$$\delta_f = ([CO_2]_a/[CO_2]_f)(\delta_a - \delta_r) + \delta_r. \tag{3.13}$$

From Eq. (3.13), it can be seen that a plot of $1/[CO_2]_f$ against δ_f gives a straight-line relationship with slope $[CO_2]_a(\delta_a - \delta_r)$, and intercept δ_r. This relationship can be applied to estimate the isotopic composition of CO_2 respired by plants and soil if data are available from at least two heights in the forest canopy.

These kinds of isotopic analyses have been applied to a number of undisturbed forests throughout the growing season and during dormant periods when evergreen forests still hold leaves but deciduous forests do not. During the growing season, in a wide variety of evergreen and deciduous types, more than 70% of the respired carbon appears derived from autotrophic respiration (Flanagan *et al.,* 1997b). Because of turbulent conditions present during the daytime, less than 5% of respired carbon appears to be reincorporated through photosynthesis, even in dense tropical forests (Buchmann *et al.,* 1997). Seasonally, the efflux of CO_2 from evergreen and deciduous forests shows different isotopic patterns as a result of the absence of any leaf photosynthesis by deciduous forests during the dormant season. These isotopic analyses are particularly valuable when combined with continuous eddy-flux and chamber measures of CO_2 and water vapor exchange.

V. MODELING PHOTOSYNTHESIS AND RESPIRATION

A. Gross and Net Photosynthesis

With an understanding of the underlying processes by which water vapor and carbon dioxide are exchanged from forest ecosystems, there is an opportunity to compare model predictions against eddy-flux measurements and to learn what simplifications can be made if the time scale of interest is expanded. As an example, we note analyses of measurements made at Harvard Forest in Massachusetts. The forest is composed of 75% deciduous hardwoods and 25% evergreen conifers. At the forest, eddy-flux data have been acquired continuously over a number of years (Wofsy *et al.,* 1993; Goulden *et al.,* 1996).

Williams *et al.* (1996) developed a fine-scale, soil–plant–atmosphere canopy model which incorporates the Farquhar model of leaf-level net and gross photosynthesis (Farquhar and Sharkey, 1982; Farquhar *et al.,* 1989) and the Penman–Monteith equation to determine leaf-level transpiration and evaporation (Monteith and Unsworth, 1990). The two process models were linked by a model of stomatal conductance (g_s) that optimized daily C gain per unit of leaf N, with limitations imposed by canopy water storage and soil-to-canopy water transport. The model assumed that the maximum carboxylation capacity (V_{cmax}) and maximum electron transport rate (J_{max}) were proportional to foliar N concentration, which changed seasonally with leaf development and senescence (Harley *el al.,* 1992; Waring *et al.,* 1995a).

The unique feature of the model lies in its treatment of stomatal opening, which explicitly couples water flow from soil to atmosphere with C fixation. The rate at which water can be supplied to the canopy is restricted by plant hydraulics and soil water availability. This rate ultimately limits transpiration because stomata close at a threshold minimum leaf water potential to prevent irreversible xylem cavitation. Because plant canopies also use water that has accumulated and been stored during periods of low transpiration (at night and when rain falls), the model optimizes carbon uptake by extracting some of the reserve of water in the morning, thus delaying the onset of stomatal closure associated with rising air vapor pressure deficits later in the day. As the canopy grows taller, hydraulic limitations on GPP are increased, but branch length was not considered.

To drive the model, meteorological data, including the fraction of direct to diffuse radiation, we required at 30-minute intervals to permit accurate estimates of irradiance through 10 canopy layers and the calculation of leaf-air vapor pressure deficits. Independent estimates of CO_2 efflux from stems and soil surface were available to allow predictions of net ecosystem exchange hourly and to model separately GPP and assimilation. Using this model, for which the required structural and environmental data were available, both hourly CO_2 exchange rate ($r^2 = 0.86$) and latent energy flux ($r^2 = 0.87$) were strongly correlated with independent whole-forest measurements obtained with eddy-flux measurements (Williams *et al.,* 1996).

Sensitivity analyses showed that major simplifications could be made in the canopy photosynthesis model, particularly if the time scale could be extended from hours to days. In forests, as we might expect, atmospheric turbulence is sufficient to allow wind speed to be set at a constant $2\,m\,s^{-1}$. The large differences in A_{max} associated with crown position were severely damped because the upper, more exposed part of the canopy was the first to suffer hydraulic restrictions that caused stomatal closure. As a result, photosynthesis was often constrained by gas diffusion before reaching light saturation.

When solar radiation was integrated over periods of a full day, the importance of distinguishing diffuse from direct solar radiation also became less important. Longer integration times, however, reduce the precision of estimates of canopy interception and could affect the accuracy of soil water balance calculations, as discussed in Chapter 2. Full-day time integration, however, significantly reduced data requirements, while still providing good agreement ($r^2 > 0.9$) with GPP estimated from hourly data (Williams *et al.,* 1996).

Jarvis and Leverenz (1983) also found, in dense Sitka spruce plantations in Scotland, that modeling of canopy photosynthesis could be simplified, without introducing much error, by assuming a linear rather than curvilinear relation with incident PAR. In more open woodlands, however, a fair proportion of the canopy may become light saturated during the day (Baldocchi and Harley, 1995). Over periods of a week to a month, however, we can assume that even forests with relatively low LAI will tend to show a linear increase in photosynthesis with absorbed PAR (Wang *et al.,* 1992a; Wang and Polgase, 1995). Of course other factors reduce potential gross photosynthesis below that predicted from light absorption alone. Landsberg (1986a) suggested that potential gross photosynthesis (GPP) be reduced on the basis of three restrictive environmental constraints to obtain an estimate of actual GPP for integration periods up to a month:

$$\text{GPP} = \alpha \ \text{APAR} \ f(\text{H}_2\text{O}) \ f(D) \ f(T) \tag{3.14}$$

where α is maximum quantum efficiency, APAR is absorbed PAR by the canopy, and modifying factors $f(i)$, which range from 1 to 0, describe reductions related to soil water deficits (H_2O), low temperature effects (T), and vapor pressure deficits of the air (D). The values of $f(H_2O)$ is reduced to zero as root zone soil water content drops below a critical point; $f(D)$ decreases linearly or nonlinearly with increasing daytime values of D. The temperature modifer $f(T)$ remains at zero for a day when temperatures drop below freezing. In essence, this calculation defines the fraction of APAR that can be effectively utilized by photosynthesis when stomata are at least partially open. McMurtrie *et al.* (1994) applied this type of analysis to 10 pine forests growing in strikingly different environments and discovered that, when deductions were made for the fraction of PAR intercepted during periods when stomata constrained CO_2 diffusion, the resulting calculation of quantum efficiency (α) approached a constant ~1.8 g C MJ^{-1} APAR.

When GPP was calculated using the simplified relation described by Eq. (3.14) with a maximum quantum efficiency during the summer of 1.65 g C MJ^{-1} APAR for the stand at Harvard Forest, predictions of GPP integrated monthly showed good agreement with GPP derived from day and night eddy-flux measurements (Fig. 3.8). Seasonal differences in canopy LAI were pronounced, and reductions in leaf chlorophyll concentrations also contributed to reducing quantum efficiency and canopy photosynthesis in the autumn (Waring *et al.,* 1995a).

In regard to our interest in scaling, we see that there are trade-offs between achieving accurate estimates of the diurnal variation in canopy photosynthesis by strata and obtaining acceptable daily or monthly estimates of photosynthesis for the entire canopy. The finer resolution models serve as excellent standards for reference and allow estimates of individual tree growth (Chapter 5), but they require much additional meteorological data and

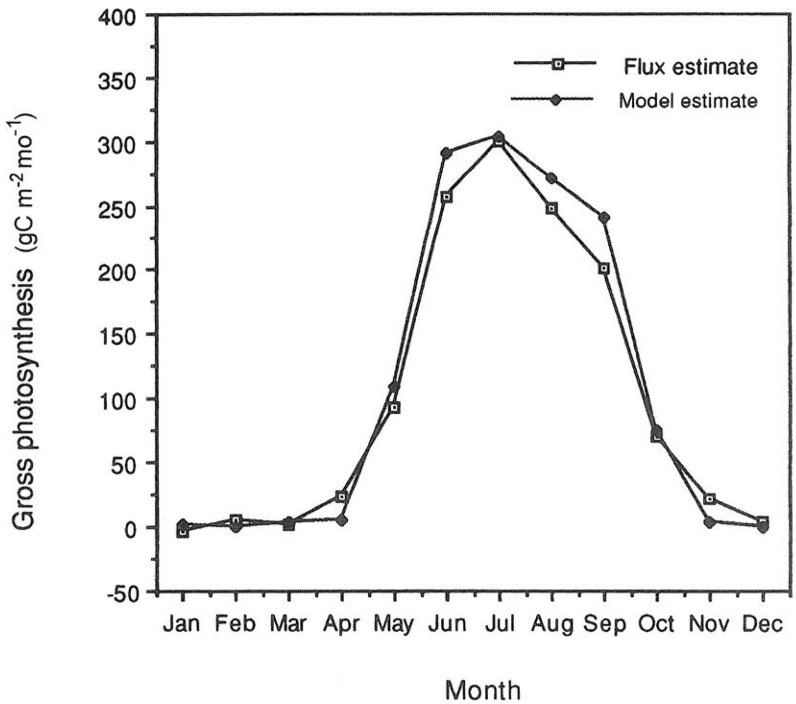

FIGURE 3.8. Monthly integrated estimates of gross photosynthesis made with a stomatal constrained quantum-efficiency model (α depended on seasonal changes in chlorophyll content of foliage but for the growing season was a constant 1.65 g C MJ^{-1} APAR) agreed well with integrated monthly values acquired from continuous flux measurements made throughout an entire year ($r^2 = 0.97$). (From Waring *et al.,* 1995a.)

detailed description of the absorption of light through the canopy. By extending the time scale of analysis from days to months there is little lost in our ability to predict whole-canopy photosynthesis. Moreover, at monthly time steps, satellite imagery is generally available to record variation in leaf area index and nitrogen status, which effectively represent the fraction of PAR that can be absorbed by all vegetation present (Sellers *et al.,* 1992a,b; Prince and Goward, 1995; Dang *et al.,* 1997; Chapters 7–9).

B. Carbon Balance of the Vegetation

If we have fairly reliable models of GPP, then they should compare well with annual estimates of the sum of carbon required for growth and autotrophic respiration. Williams *et al.* (1997) applied their daily integrated model of GPP developed at Harvard Forest to a wide range of forests in Oregon, arrayed along a 250-km transect at 44° N latitude (Table 3.3). Data on canopy LAI, foliar biomass, and N content were available from Runyon *et al.* (1994) and Matson *et al.* (1994). Predawn water potentials reached levels that might significantly constrain stomatal conductance only on sites 2, 5, and 6 (Runyon *et al.,* 1994). GPP was not measured at any of the sites but was estimated with an annual component carbon budget:

$$\mathrm{GPP} = \mathrm{NPP_A} + \mathrm{NPP_B} + R_{\mathrm{SA}} + R_{\mathrm{SB}} + R_{\mathrm{Msap}} + R_{\mathrm{Mfol}} + R_{\mathrm{Mroot}} \tag{3.15}$$

TABLE 3.3
Ecosystem Variables and Annual Environmental Variables for Sites across the Oregon Transect[a]

Site	Species	LAI	Mean foliar N (g m^{-2})	Mean annual temp. (°C)	Growing season[b] (Julian dates)	Annual total PAR (MJ m^{-2} $year^{-1}$)	Minimum ψ (MPa)	Average maximum canopy height (m)
1	*Picea sitchensis/Tsuga heterophylla*	6.4	1.2	10.1	75–320	1934	−0.5	50
1A	*Alnus rubra*	4.3	2.4	10.1	110–275	1934	−0.5	13
2	*Pseudotsuga menziesii/Quercus garryana*	5.3	1.8	11.2	75–280	2267	−1.7	40
3	*Tsuga heterophylla/Pseudotsuga menziesii*	8.6	1.7	10.6	75–305	2259	−0.5	30
4	*Tsuga metensiana/Abies lasiocarpa/ Picea engelmanii*	1.9	3.0	6.0	160–256	2088	−0.5	20
5	*Pinus ponderosa*	0.9	2.7	7.4	125–275	2735	−1.7	30
6	*Juniperus occidentalis*	0.4	5.8	9.1	125–275	2735	−2.5	10

[a]After Williams *et al.* (1997), developed from Runyon *et al.* (1994) and Matson *et al.* (1994).
[b]Growing season signifies those days when leaves are present and photosynthesis is possible. In some climates the season is abbreviated because of long periods below freezing.

where NPP_A and NPP_B are aboveground and belowground net primary production; R_{SA} and R_{SB} are aboveground and belowground synthesis respiration; and R_{MSap}, R_{Mfol}, and R_{Mroot} are, respectively, sapwood, foliage, and fine-roots maintenance respiration. NPP_A includes new foliage production and branch and stem growth. Runyon *et al.* (1994) provided estimates of these quantities from equations related to annual increases in stem diameter determined from extracted wood cores. Belowground net primary production (NPP_B) was not measured; instead, the relationship based on litterfall (Raich and Nadelhoffer, 1989; Fig. 3.6) was applied. Ryan *et al.* (1995) provided estimates of sapwood maintenance respiration at site 3 (western hemlock, Douglas-fir); the annual value was around 5% of estimated GPP (Fig. 3.5). For the other sites, Williams *et al.* assumed a similar ratio of R_{Msap} to NPP_A (18%). Foliage respiration (R_{Mfol}) was determined from total canopy N and daily and seasonal variations in temperature following the approach developed by Ryan (1991b, 1995).

Daily climatic data from the site meteorological stations were used to run the unmodified Harvard Forest model through the annual cycle to estimate GPP. On days that temperature dropped below −2°C, no C fixation was assumed to occur as a result of frost. LAI in the coniferous stands varied by around 30% each year (Runyon *et al.,* 1994), and its seasonal variation was taken into account. Foliar N concentrations, however, were assumed constant throughout the year, except for the deciduous forest. Predawn water potentials below −1.5 MPa were assumed to cause complete stomatal closure, except for the more drought-resistant *Juniperus occidentalis,* where limits were set at −2.5 MPa. GPP estimates obtained with the simulation model (Williams *et al.,* 1996, 1997) compared well with those calculated with Eq. (3.15) ($r^2 = 0.97$; Fig. 3.9a). The only exception was at site 1, where an old-growth forest exhibited greater hydraulic restrictions of water flow than the model assumed (Chapter 2).

An important insight gained from constructing the carbon balances for the stands distributed across the Oregon transect was that the ratio of NPP/GPP is conservative, averaging 0.46 with a total range from 0.40 to 0.52. Additional comparisons were added from similar carbon balance analyses made at Harvard Forest (Williams *et al.,* 1997), at three pine plantations in Australia (Ryan *et al.,* 1996b), and in a native *Nothofagus* forest in New Zealand (Benecke and Evans, 1987), and all showed that the ratio NPP/GPP remains essentially constant (Fig. 3.9b). The finding that NPP/GPP is a conservative ratio has been reported previously in growth room studies where respiration and photosynthesis have been monitored for short periods on a variety of species exposed to a range of temperatures from 15° to 30°C (Gifford, 1994). The balance between photosynthesis, respiration, and growth could reflect the key role of nitrogen, as will be discussed in later sections. The NPP/GPP ratio is relatively conservative but may be significantly lower in boreal forests (~0.25) than in other biomes (Ryan *et al.,* 1997a).

C. Assessment of Heterotrophic Respiration

Although heterotrophic respiration may be a relatively small component of total ecosystem respiration under undisturbed conditions, it is a critical component and one that could change measurably with disturbance or climatic warming. In a steady-state condition, one

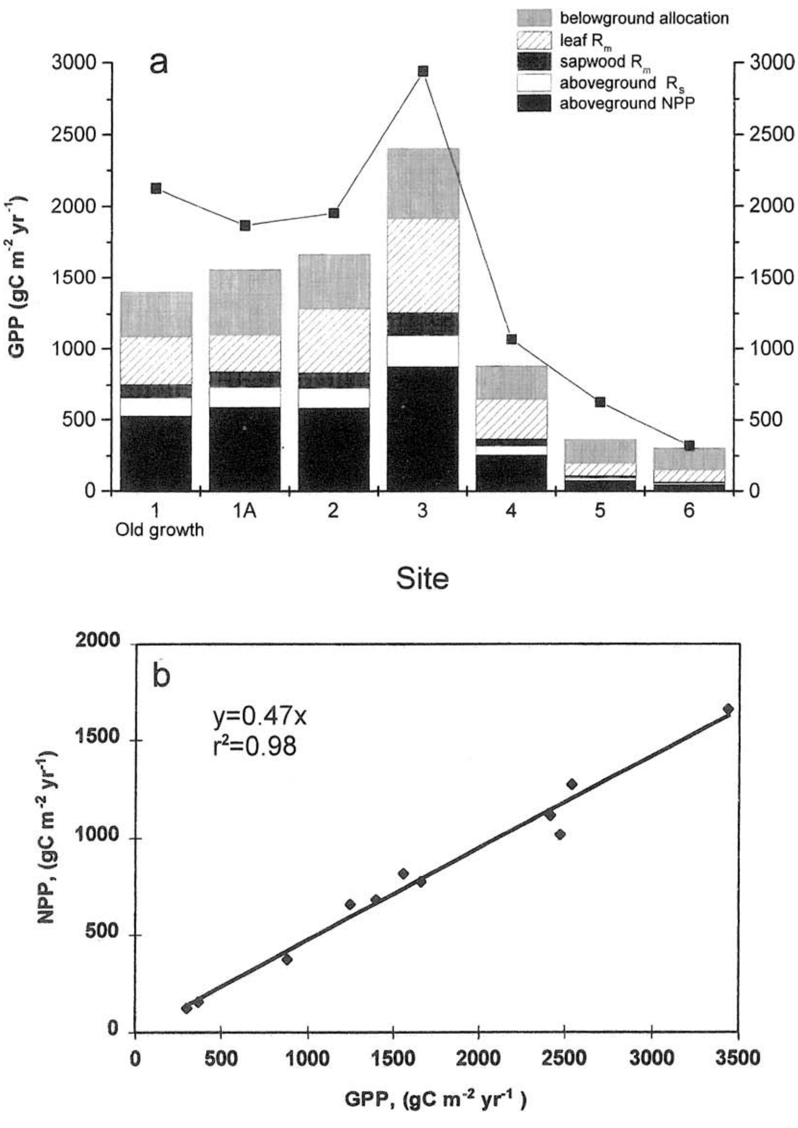

FIGURE 3.9. (a) For seven sites across the Oregon transect, GPP (■) estimated with a daily resolution process model is compared with a component analysis that sums to GPP (stacked bars). The dominant species at each site are given in Table 3.3. (Provided by Mathew Williams, personal communications, with data from Williams *et al.,* 1997.) (b) The ratio NPP/GPP, determined by component carbon balance analyses, is essentially constant for a dozen forests that include seven on the Oregon transect (Williams *et al.,* 1997), three pine plantations in Australia (Ryan *et al.* 1996b), Harvard Forest (Williams *et al.,* 1997), and a *Nothofagus* forest in New Zealand (Benecke and Evans, 1987). Regression of NPP to GPP has been forced through the origin. The slope of the relation is 0.47 with a standard deviation of 0.04 for temperate forests analyzed in Table 3.3. (After Waring *et al.,* 1998.)

might expect on an annual basis that heterotrophic respiration might approach a fixed fraction of total ecosystem respiration and GPP, and certainly total soil respiration is closely related to NPP (see global review paper by Raich and Schlesinger, 1992). Steady-state conditions, however, rarely apply, as demonstrated at Harvard Forest where continuous eddy-flux measurements were made over a 5-year period. When the total respiration ($R_a + R_h$) was compared as a fraction of GPP it averaged 0.82 but varied from 0.75 to 0.90 (Goulden *et al.,* 1996). With more detailed studies, Goulden *et al.* found, during an extended period of drought, that heterotrophic respiration decreased much more than photosynthesis and autotrophic respiration. Because heterotrophic respiration is largely confined to the surface litter and upper soil horizons that dry quickly, R_h is very responsive to drought, whereas R_a is less sensitive because few perennial roots actually die as a result of drought (Marshall and Waring, 1985) and because fine-root growth continues in the lower soil horizons where water is still available.

Modeling seasonal variation in soil respiration realistically requires the recognition of at least three distinct horizons: surface litter, surface soil, and the deeper rooting zone. We can expect this level of definition, or even finer, to apply in predicting the seasonal availability of soil nutrients to plants (Chapter 4). It is clear why we require seasonal resolution and some underlying understanding of basic processes to provide an alternative to long-term monitoring and to allow, where possible, simplifications that are justified from more detailed spatial and temporal analyses. One promising example of the application of a coupled ecosystem model (FOREST-BGC) is its ability to predict the separate components of carbon acquisition and loss in forests other than those where it was originally developed (Fig. 3.10). In a later section we will compare and contrast the structure and function of other dynamic ecosystem models that generate seasonal estimates of fluxes (C, H_2O, and N).

VI. NET PRIMARY PRODUCTION AND ALLOCATION

The amount of carbon that may be synthesized into new tissues, storage reserves, and protective compounds is determined from the photosynthate remaining after accounting for autotrophic respiration ($R_m + R_s$). Partitioning of assimilate into various products and the biochemical composition of those products are affected by the relative availability of critical resources (solar energy, water, nitrogen, CO_2, and temperature). From an evolutionary perspective, carbon products synthesized by plants might be expected to increase the chances of an individual tree and its progeny surviving. Species differ, however, in their adaptations and thus in the way carbon and other resources are allocated. For example, some pine species produce serotinous cones that provide viable seeds following a destructive fire. In contrast, redwood and eucalyptus respond to fire by producing epicormic branches from their main stems.

In this section we first describe how trees allocate assimilated carbon seasonally. A set of concepts is introduced that have served as a basis for modeling seasonal shifts in allocation. Simpler analyses are introduced for assessing annual patterns. With some understanding of why allocation patterns shift, we define a number of indices which reflect responses of trees to competition in general as well as to specific stresses. These allocation indices provide a means of interpreting how different tree species and whole forests are likely to respond to changing environmental conditions, seasonally as well as over their life span.

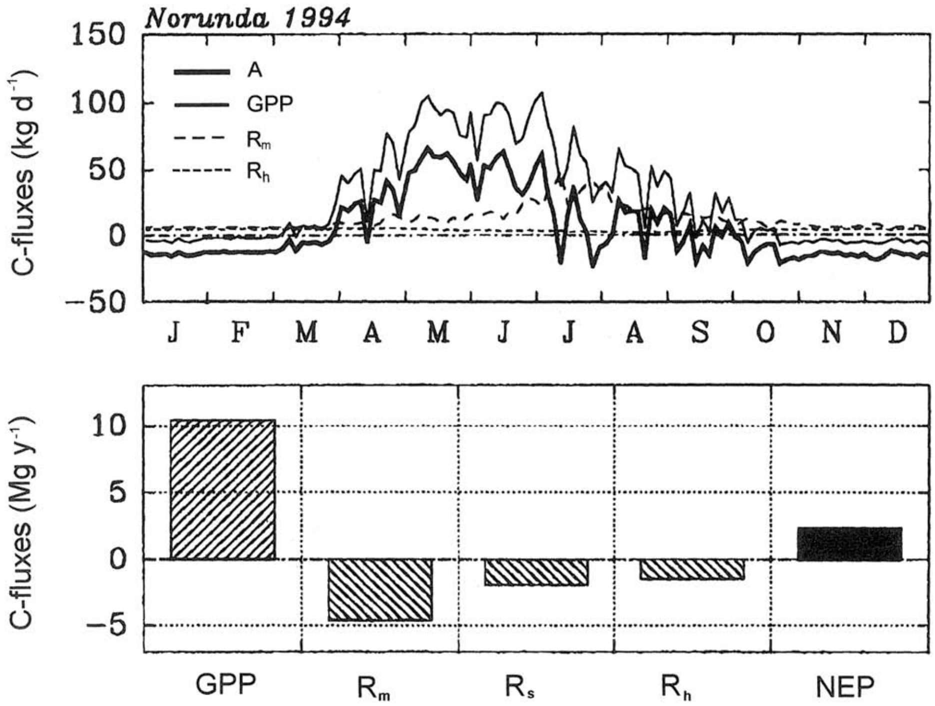

FIGURE 3.10. Net ecosystem CO_2 fluxes were measured continuously with eddy-flux instrumentation at the NOPEX site in central Sweden above a 25-m-tall spruce and pine forest which had a range in LAI between 3 and 6. Simulation of the components of net ecosystem production [assimilation, *A;* gross primary production, GPP, maintenance respiration, R_m, heterotrophic respiration, R_h, and growth (synthesis) respiration, R_s] were estimated with FOREST-BGC. (Reprinted from *Journal of Hydrology,* E. Cienciala, S. W. Running, A. Lindroth, A. Grelle, and M. G. Ryan, "Analysis of carbon and water fluxes from the NOPEX boreal forest: Comparison of measurements with FOREST-BGC simulations," 1998, with kind permission of Elsevier Science–NL, Sara Burgerhartstraat 25, 1055 KV Amsterdam, The Netherlands.)

A. Seasonal Dynamics in Allocation

In perennial plants, and particularly long-lived trees, there is much seasonal variation in NPP and its allocation (Mooney and Chu, 1974). Generally, we can consider that no growth or storage of carbohydrates occurs until the basal metabolic requirements for all living cells are first met. Storage reserves must be present to cover maintenance costs during the night and other nonphotosynthetic periods. These key limitations on allocation of reserves are usually applied in process models designed to predict seasonal growth patterns (Cannell and Dewar, 1994).

In favorable climates, where growth may be continuous, allocation patterns might be assumed fixed, and growth rates would then be proportional to the pool of carbohydrates available. In reality, the growth of reproductive organs, roots, and shoots is rarely in phase. Internal controls on allocation are hormonal, but they reflect evolutionary adaptations to climatic, edaphic, and biotic pressures. At present, the allocation process is very poorly understood in comparison to photosynthesis, yet it is critically important because a 5% shift in allocation away from fine-root production may permit a 30% increase in foliage mass (Cropper and Gholz, 1994).

A number of schemes have been proposed to model carbon allocation, as summarized by Cannell and Dewar (1994). They postulate that (i) photosynthate is allocated from sources in accordance with assigned sink strengths (Ford and Kiester, 1990; Luxmoore, 1991; Thornley, 1991); (ii) photosynthate is allocated to points where a resource deficiency first occurs (Ewel and Gholz, 1991); (iii) plants maintain a functional balance between carbon fixation by shoots and nutrient and water uptake by roots (Davidson, 1969); (iv) carbohydrates are dispersed in proportion to distance from the site of fixation, and nutrients and water are allocated in the opposite order (Weinstein *et al.,* 1991); and (v) carbon is allocated to optimize net carbon gain or total plant growth rate (Ågren and Ingestad, 1987; Johnson and Thornley, 1987). The various assumptions on allocation are interrelated; however, none deals fully with underlying processes, and some are in direct conflict with one another. Even within one scheme (scheme v), Thornley's model assumes that sink strength is controlled by carbon and nitrogen substrate concentrations, whereas Ågren and Ingestad (1987) define sink strength based on the total nitrogen content in the canopy.

Models that relate root uptake of nitrogen and shoot uptake of carbon have progressed slowly toward more realistic assumptions (Fig. 3.11). Initially, growth was assumed to be a simple function of the amount of carbon and nitrogen available, with the product of carbohydrate and nitrogen resources in foliage and roots determining the relative allocation. More refined models include resistance to transport and demands for resources by intermediate structures between roots and shoots. More mechanistic models consider sugar and amino acid transport separately through phloem and sapwood (Cannell and Dewar, 1994). Root-to-shoot gradients in water potential also influence the rates at which resources are transported through the two vascular systems (Dewar, 1993).

Carbon allocation models apply particularly well to species showing *indeterminate* growth. In many forests, however, trees are dormant in certain seasons, independent of the amount of carbohydrates or nitrogen available. For example, at full leaf, an oak tree may have accumulated sufficient starch reserves to replace its canopy three times (McLaughlin *et al.,* 1980). The seasonal timing of growth (*phenology*) must be predicted or continuously monitored.

Plant phenology has been correlated with a variety of environmental signals. In tropical or desert regions, the onset of a wet season (or sometimes the end of a dry season) may initiate conditions favorable for growth (Borchert, 1973; Reich, 1995). In boreal and temperate regions, day length and temperature are major controlling variables, with different species exhibiting different genetically programmed thresholds. Shorter day lengths, or, more precisely, longer nights, induce dormancy, whereas longer day lengths induce hormonal changes that favor growth. Cessation of growth and senescence of leaves may also be triggered by drought or subfreezing temperatures. Growth in temperate, subalpine, and boreal zones is not initiated until soil temperatures rise at least a few degrees above freezing. A number of empirical models predict budbreak, elongation, and budset on the basis of accumulated daily temperature values (heat sums) above some minimum threshold temperature (Hari and Hakkinen, 1991; Dougherty *et al.,* 1994; Whitehead *et al.,* 1994). Other phenology models integrate soil and air temperature values to predict leaf and stem

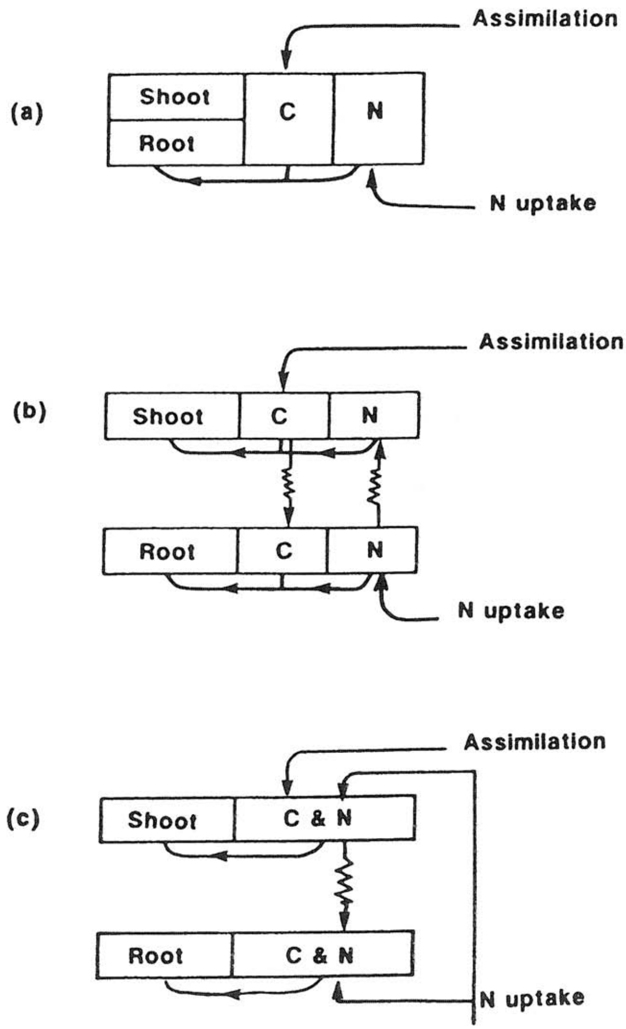

FIGURE 3.11. Progressively more sophisticated allocation models are presented from top to bottom. In (a) partitioning of assimilate is determined by the product of carbon (C) and nitrogen (N) concentrations in roots or shoots. In (b) opposite gradients in C and N are envisioned between shoots and roots with resistances against transport in both directions. In (c), transport of C and N are both considered to be through the phloem, which is the most realistic model and accommodates changes in plant water relations. (From Dewar *et al.,* 1994.)

phenology (Cleary and Waring, 1969). With daily satellite imagery now available, the phenology of vegetation can be assessed by observations at regional and global scales (Chapters 7–9).

With knowledge of phenology and environmental conditions, the pools of available carbon and nitrogen can be allocated into biomass, storage reserves, and losses through respiration. Weinstein *et al.* (1991) generated seasonal estimates of carbon allocation for red spruce by assuming priorities based on proximity to the resource (scheme iv; Fig.

3.11b). In this model, leaf growth had first priority for carbon after maintenance requirements of all living tissue were met. Storage of carbon in leaves had the next priority, followed by growth and storage in branches, stem, coarse roots, and, last, fine roots. Carbon in excess of that needed to meet the maximum growth rate of an organ was passed down the priority chain. The priority ranking for allocation of water and nutrients would, according to this proximity logic, be the opposite, with fine roots ranked first and new foliage ranked last. Because critical resources come from opposite directions, no given organ is likely to grow at its full potential, unless phenology limits all growth elsewhere. Predictions of photosynthate allocation seasonally in *Picea rubens,* based on phenology and the proximity logic (Fig. 3.12), showed reasonable growth patterns and matched measured storage reserves within 10% and total carbon content within 2% at the end of the year (Weinstein *et al.,* 1991). Most seasonal models of carbon allocation require specific knowledge of plant phenology, definition of the limits to growth of various organs, and specification of the size of storage reserves in all major organs.

B. Annual Assessment of NPP Allocation

Annual changes in carbon allocation are much easier to assess and to model than seasonal patterns. Annual primary production represents all carbon sequestered into dry matter during a year and is equivalent to total carbon uptake through photosynthesis minus the loss through autotrophic respiration. In practice, net primary production (NPP) is estimated

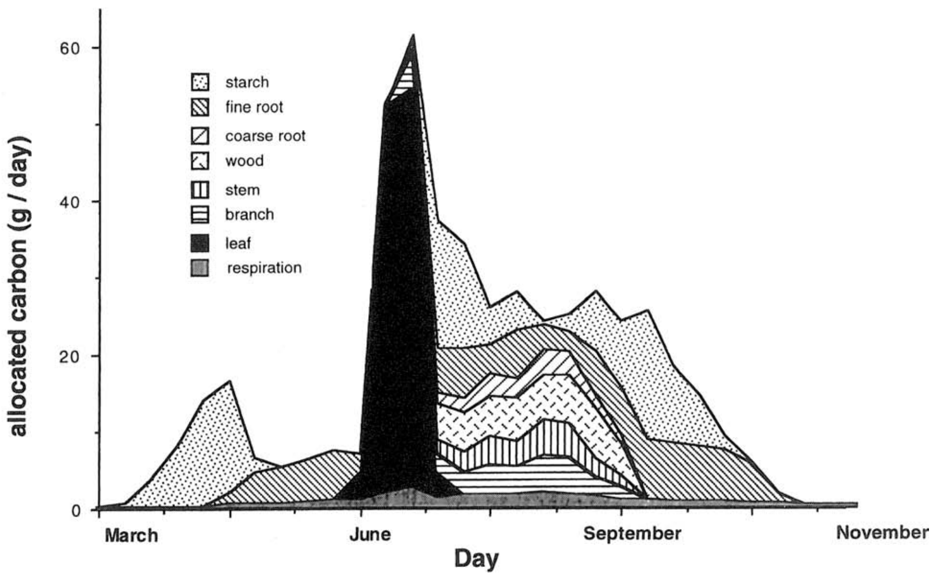

FIGURE 3.12. Seasonal carbon allocation patterns generated with a simulation model for red spruce (*Picea rubens*) are dependent on phenology and proximity to resources. Starch reserves accumulate when growth is at a minimum compared to photosynthesis. Leaf growth attains priority in June while the production of other structural components peaks thereafter. (After Weinstein *et al.*, 1991.)

by summing the growth of all tissue produced during a year, whether or not the tissue was consumed by herbivores or entered the detrital pool. The equation is

$$\mathrm{NPP} = \Delta B + D_{\mathrm{B}} + C_{\mathrm{B}} \tag{3.16}$$

where ΔB is the change in biomass over a period of a year, D_{B} is detritus produced during the year, and C_{B} represents consumption of biomass by herbivores during the year.

Consumption by animals is usually a small fraction of total NPP in forests unless there is an outbreak of defoliating insects (Chapter 6). Even if 10% of the foliage is consumed, this represents less than 3% of total NPP in deciduous or evergreen forests. Estimates of foliage consumption are made by deducting the area of sample leaves that are partially consumed (Reichle *et al.,* 1973) relative to comparable foliage on twigs that developed normally, or by measuring insect frass in litterfall traps and calculating the weight of tissue consumed to produce the amount of frass. Animals also eat roots and fruits, but this consumption is ignored in most calculations of NPP in forests.

From destructive analysis of trees, information can be obtained on how growth is distributed. In a particular climatic zone, the annual pattern of carbon allocation to foliage and stem wood shows a general consistency (Fig. 3.13a), except when large crops of seeds are produced or unusual weather conditions prevail (Eis *et al.,* 1965; Pregitzer and Burton, 1991). Proportional increments in biomass of stem wood, leaves, branches, and large-diameter roots are related exponentially to increases in stem diameter (Whittaker and Woodwell, 1968; Kira and Ogawa, 1971; Gholz *et al.,* 1979; Deans, 1981; Pastor *et al.,* 1984; Fig. 3.13b). *Allometric* relations derived from such analyses allow computation of forest biomass and also the estimation of stores of carbon and nutrients in various components as forests grow (Chapter 5). Production is determined by periodic measurement of stem diameter or by extracting wood cores and measuring annual increments. Biomass and production of shrubs and herbs in forest undergrowth are estimated separately, often by obtaining correlations with cover which can be estimated with increasing accuracy using digital imagery acquired from the ground and from satellites (Levine *et al.,* 1994; Law, 1995). Biomass increment is calculated by measuring all trees within a known area or by using variable-plot surveys based on the diameter of trees intercepted by a selected angle. Variable-plot surveys are generally more efficient because only a few trees require measurement at each sampling point (Sukwong *et al.,* 1971).

Soil organic matter consists of fresh litter, partially decomposed material, and humus. The total dead organic matter in an ecosystem is sometimes called "detritus," although we prefer to restrict the term to dead material from which the source can still be recognized. The annual loss of leaves, twigs, flowers, fruits, and bark fragments represents the obvious forms of litterfall in forest ecosystems. Leaf litter typically makes up 70% of the total annual litterfall from above ground that is collected in litter screens (Waring and Schlesinger, 1985). The composition and quantity of litterfall are often variable between years. During insect outbreaks the production of frass may represent more than the annual production of foliage in evergreen forests (Chapter 6). The resulting dead trees disappear much more slowly than leaves from an ecosystem, and in their slow decay they play special roles that will be described in Chapter 5.

In this chapter, we consider the smaller detrital components which consist mainly of leaf litter, twigs, and small-diameter roots that die and accumulate throughout a year on

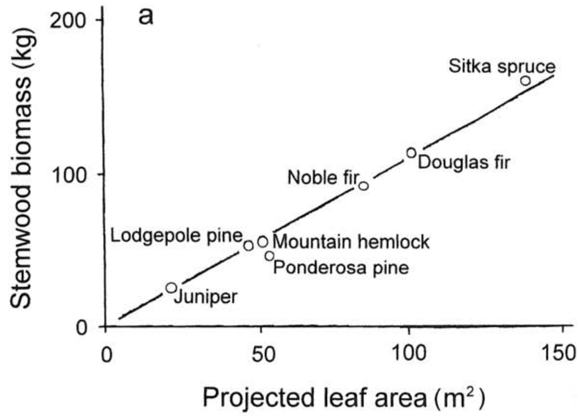

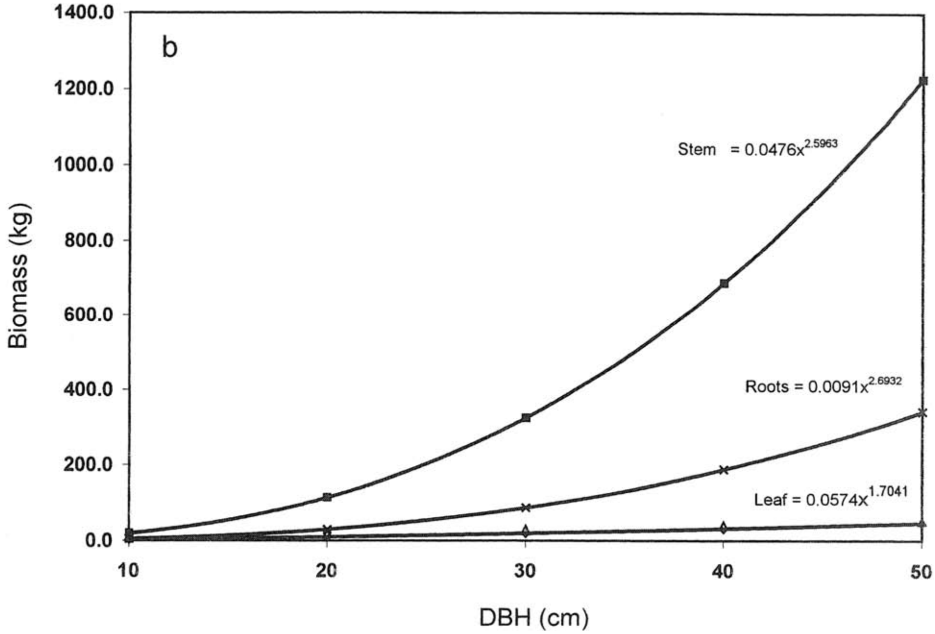

FIGURE 3.13. (a) For conifers distributed across a steep environmental gradient in Oregon, trees of a comparable diameter, here 20 cm, show an increase in stem wood mass and projected leaf area (derived from leaf area/sapwood area relationships) that reflects a transition from the most extreme dry and cold environments supporting *Juniperus* toward a mild, frost-free, and moist coastal environment where Sitka spruce (*Picea sitchensis*) is restricted. Variation occurs in these allometric relations for species such as *Pinus ponderosa* and Douglas-fir (*Pseudotsuga menziesii*) with wide environmental ranges. (After Waring, 1980.) (b) Allometric relations developed for Douglas-fir growing in western Oregon show that the biomass of stems, roots, and leaves increases exponentially with stem diameter (x, cm) at breast height (DBH). Equations were transformed from natural log–linear relationships presented by Gholz *et al.* (1979).

the soil surface or within the soil. Aboveground estimates of litterfall are obtained by installing sets of screens to catch material which is then weighed. The smaller diameter roots (0.5 to 5 mm) which are produced within a year usually die and begin to decompose (Harris *et al.,* 1975; McGinty, 1976; Persson, 1978). The smaller the diameter of a root, the shorter is its life span (Schoettle and Fahey, 1994). Typically, estimates of fine-root production and turnover have been obtained by comparing seasonal changes in the standing crop of live roots extracted from soil cores (Fig. 3.14). A large number of samples is required to reduce the standard error of the estimate to less than 10%, and a bias to overestimation is common (Singh *et al.,* 1984; Kurz and Kimmins, 1987; Schoettle and Fahey, 1994). Nondestructive measures of root growth and turnover have been obtained by analyzing sequential digital images of the same soil surface acquired with miniature video cameras inserted in root periscopes (Olsthoorn and Tiktak, 1991; Hendrick and Pregitzer, 1993; Reid and Bowden, 1995).

As mentioned previously, the total carbon allocated to roots may also be estimated indirectly through a correlation with litterfall and CO_2 efflux from the soil (Raich and Nadelhoffer, 1989; Hanson *et al.,* 1993). Temperature is assumed to have a similar influence on root and microbial activity in the relationship. This assumption may be unwarranted, however, because of interactions with the depletion of surface soil water and because of the ability of fine roots to respire as long as they have starch or other reserves to expend (Marshall and Waring, 1985).

Much additional insight has been gained by a few groups who established plantations of trees in one area and then experimentally manipulated the availability of resources to quantify shifts in carbon allocation (Linder, 1986; Linder *et al.,* 1987). These kinds of experiments have, along with eddy-flux measurements, greatly advanced our abilities to

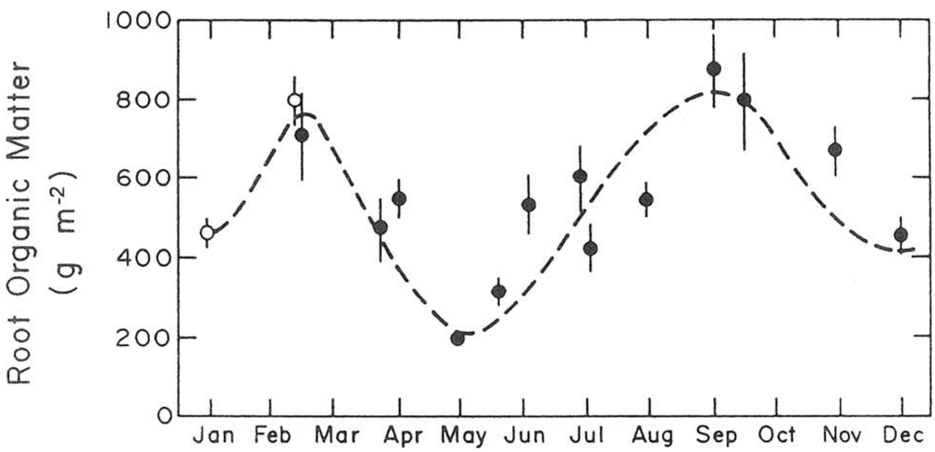

FIGURE 3.14. Seasonal changes in the standing crop of small-diameter roots in a *Liriodendron* forest were obtained by core samples collected throughout the year. Estimates of production and turnover rates are obtained from differences in peak and nadir biomass. Organic matter production in this case was about 1460 g m^{-2} year^{-1} with an average standing crop of 680 g m^{-2}. (After "Carbon cycling in a mixed deciduous forest floor" by N. T. Edwards and W. F. Harris, *Ecology,* 1977, **58**, 431–437. Copyright © 1977 by the Ecological Society of America. Reprinted by permission.)

generalize and model ecosystem responses. As an example, we cite a long-term study initiated on a *Pinus radiata* plantation in Australia described in more detail by Landsberg (1986b) and Benson *et al.* (1992). Treatments applied to the pine plantation were irrigation, fertilizer without irrigation, and fertilizer plus irrigation with a balanced nutrient solution, along with the untreated "control." Some results of this experiment (Table 3.4) show that significant shifts occurred in allocation and respiration by trees subjected to the different treatments. Irrigation increased aboveground and fine-root growth by about 25%, without increasing leaf area index above that of the untreated control. It was assumed that photosynthetic rate decreased as leaf N concentrations fell from 1.3% in the control to 1.1% with irrigation (Ryan *et al.*, 1996b). Addition of water and nutrients together resulted in a 40% increase in GPP and a 150% increase in foliage production, raising LAI to 4.6. Stem and coarse-root production in the irrigation plus fertilizer treatment increased by a similar amount to that observed with irrigation alone. The analysis indicates that with irrigation and fertilization about 10% of GPP was expended on fine roots and mycorrhizae, whereas in the irrigated treatment the allocation to these components reached 30% of GPP.

Similar results have been observed in other studies (Alexander and Fairly, 1983; Beets and Whitehead, 1996). Although the precision of estimates varied, with less accuracy in the fraction of carbon allocated below ground, the sum of all estimates of growth and

TABLE 3.4
Annual Carbon Budget of *Pinus radiata* Stands in Australia with Different Treatments[a]

	C (Mg ha^{-1} year^{-1})		
Variable	Control	Irrigated	Irrigated and fertilized
Foliage production	0.84	1.13	2.13
Foliage R_s	0.21	0.28	0.53
Foliage R_m	4.00	2.67	6.28
Branch production	0.22	0.22	0.27
Branch R_s	0.05	0.05	0.07
Branch R_m	1.11	1.20	1.87
Stem + bark production	4.93	6.15	10.51
Stem + bark R_s	1.23	1.54	2.63
Stem wood R_m	1.34	1.71	2.70
Aboveground NPP	(*5.99*)	(*7.50*)	(*12.91*)
Coarse-root production	1.19	1.56	2.96
Coarse-root R_s	0.30	0.39	0.74
Coarse-root R_m	0.50	0.64	1.24
Fine-root production	1.85	2.35	1.33
Fine-root R_s	0.46	0.59	0.33
Fine-root R_m	1.48	1.47	1.42
Mycorrhizae + exudates	4.43	3.36	–0.63
Total belowground allocation, B_a	(10.21)	(10.36)	(7.39)
Gross primary production	24.14	25.31	34.38

[a]Respiration is partitioned into components: synthesis (R_s) and maintenance (R_m). Total belowground carbon allocation was estimated as the difference between annual soil respiration and aboveground litterfall plus coarse toot increment. Mycorrhizae or root exudation was estimated as the difference between B_a and root respiration plus production. After Ryan *et al.* (1996b).

autotrophic respiration averaged within 10% of annual simulated gross photosynthesis (Ryan *et al.,* 1996b). If these analyses are correct, fine-root production, including the support of mycorrhizae, might be expected to represent between 10 and 60% of total NPP (Ryan *et al.,* 1996b; Beets and Whitehead, 1996). From similar but more extensive analyses performed on other pine plantations, Beets and Whitehead (1996) demonstrated that by increasing the availability of nitrogen, the annual fraction of NPP allocated to fine roots decreased from 60 to about 10% (Fig. 3.15a), while the fraction allocated to stem wood

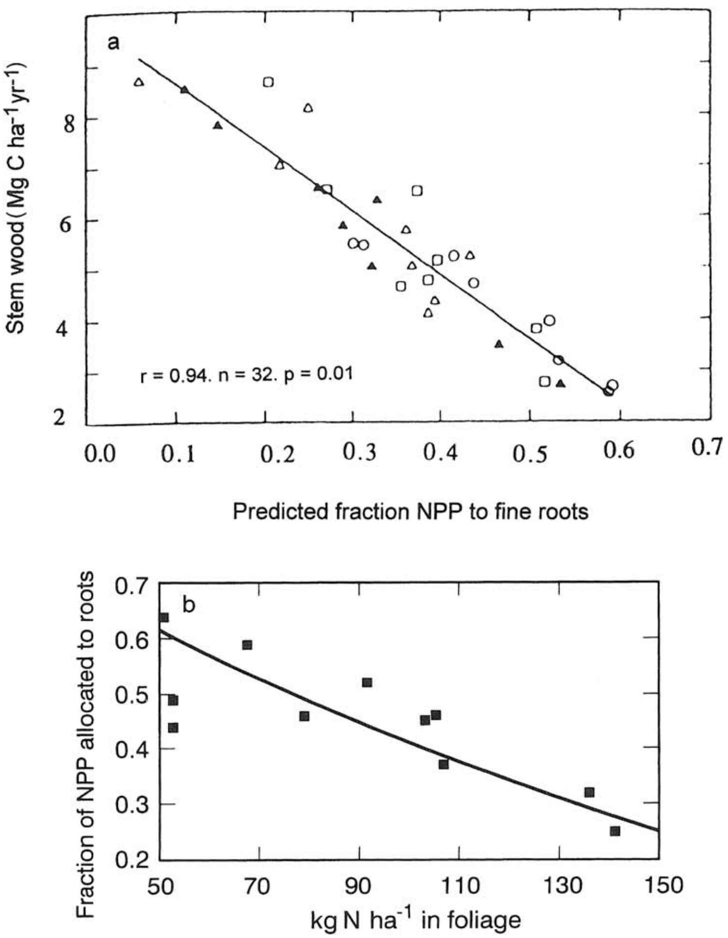

FIGURE 3.15. (a) Increasing the availability of nitrogen to *Pinus radiata* plantations in New Zealand did not change the concentration of N in foliage, but it caused a proportional shift in carbon allocation of NPP away from fine roots into stem wood. Root production was estimated from a component analysis as a residual. (From Beets and Whitehead, 1996.) (b) As the total content of nitrogen in the radiata pine canopy increased from 50 to nearly 150 kg N ha^{-1}, the fraction of NPP allocated to all roots showed a decrease from a maximum of about 0.65 to a minimum of about 0.25. Graph was made from a composite of information collected by Beets and Madgwick (1988) and from Beets and Whitehead (1996). (Modified from *Forest Ecology and Management,* Volume 95, J. J. Landsberg and R. H. Waring, "A generalized model of forest productivity using simplified concepts of radiation-use efficiency, carbon balance and partitioning," pp. 209–228, 1997, with kind permission of Elsevier Science–NL, Sara Burgerhartstraat 25, 1055 KV Amsterdam, The Netherlands.)

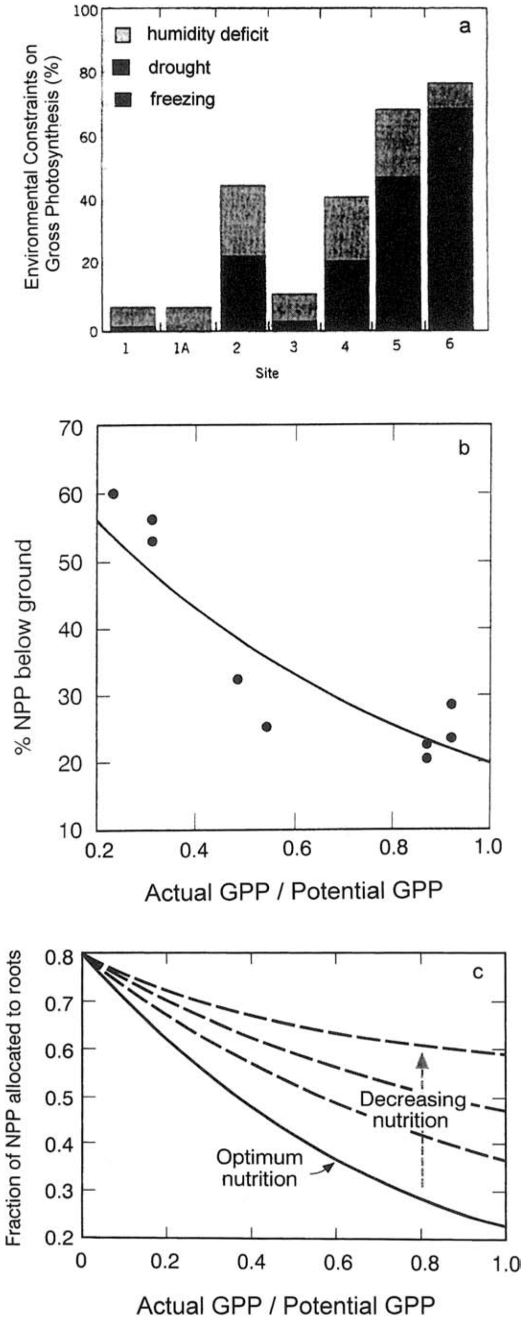
a
humidity deficit
drought
freezing
Environmental Constraints on Gross Photosynthesis (%)
Site
1
1A
2
3
4
5
6
b
% NPP below ground
Actual GPP / Potential GPP
c
Fraction of NPP allocated to roots
Decreasing nutrition
Optimum nutrition
Actual GPP / Potential GPP

and leaf area increased proportionally. If only nitrogen were a limiting factor, the allocation could be predicted from a correlation between total foliage N content and the proportion of carbon allocated to all sizes of roots, with the remaining NPP going to aboveground growth (Fig. 3.15b). Deficiencies in nitrogen, and to a lesser extent phosphorus and sulfur, favor growth of small-diameter roots over that of shoots, whereas deficiencies in potassium, magnesium, and manganese have the opposite effect (Wikström and Ericsson, 1995). Nutrient imbalances in general require plants to expend more energy and reduce overall growth (Sheriff *et al.,* 1986; Schulze, 1989).

In addition to limiting nutrients, dry soils and restrictive temperatures, as mentioned earlier, may result in an increase in the fraction of NPP allocated below ground. Across the Oregon transect, where a combination of factors limited stomatal conductance (Fig. 3.16a), the fraction of NPP allocated to roots varied over a similar range to that observed in Fig. 3.15a and was correlated with the ratio of actual GPP to potential GPP (Fig. 3.16b).

The relative importance of climatic and edaphic limitations of carbon allocation to roots should change seasonally. As the ratio GPP/potential GPP approaches unity, soil fertility will play an increasingly important role, with the most infertile soils requiring the maximum fraction of NPP allocation under otherwise favorable environmental conditions (Fig. 3.16c).

Landsberg and Waring (1997) applied this reasoning in the construction of a stand growth model with monthly time steps that contained the following simplifying assumptions: (a) potential GPP is a linear function of APAR (1.8 g C MJ^{-1}), (b) actual GPP reflects additional environmental constraints that limit diffusion of CO_2 through stomata, (c) NPP is 45% of GPP, and (d) the fraction of NPP to roots varies depending on the monthly calculated ratio GPP/potential GPP. The remaining NPP not allocated to roots was proportioned into foliage and stem production on the basis of the ratio of the rate of change in weight of foliage to the rate of change in stem biomass determined with species-specific allometric equations (McMurtrie and Wolf, 1983; McMurtrie and Landsberg, 1992). The model reduced the fraction of NPP allocation to leaves when environmental conditions favored root growth and resulted in a net decrease in LAI when monthly production of leaves was less than a set value for leaf litterfall. Model predictions of annual aboveground stem biomass for two *Pinus radiata* plantations agreed almost 1 : 1 with measured values

---

FIGURE 3.16. (a) The environmental constraints on gross photosynthesis vary across the Oregon transect depending on limitations from humidity deficits, drought, and freezing. The forest types include old-growth Sitka spruce (1) and alder (1A), mixed forests of conifers with deciduous oak (2), fast-growing Douglas-fir and western hemlock on the western slopes of the Cascade Mountains (3), a subalpine forest (4), an open pine forest (5), and juniper woodland (6). (From Runyon *et al.*, 1994.). (b) With increasingly climatic constraints on photosynthesis across the Oregon transect, the ratio of actual GPP/potential GPP falls and, with it, the fraction of NPP allocated belowground annually. (After Runyon *et al.,* 1994.) (c) The ratio actual GPP/potential GPP controls the minimum fraction of NPP allocated to roots in a growth model with monthly resolution. The additional possible constraints of limiting nutrition are incrementally added. In months favorable for photosynthesis, the model shows the greatest effect of nutrition on allocation. As environmental conditions become progressively less favorable, the availability of nutrients has a decreasing effect on allocation. (Modified from *Forest Ecology and Management,* Volume 95, J. J. Landsberg and R. H. Waring, "A generalized model of forest productivity using simplified concepts of radiation-use efficiency, carbon balance and partitioning," pp. 209–228, 1997, with kind permission of Elsevier Science–NL, Sara Burgerhartstraat 25, 1055 KV Amsterdam, The Netherlands.)

acquired annually over periods up to 30 years, when harvesting begins, taking into account natural mortality predicted with a self-thinning rule that will be discussed in Chapter 5.

For scaling principles, the approach outlined above has several lessons. First, simplifying assumptions must be derived from comparative studies across a range of environments and forest conditions. Second, a minimum time step must be identified (e.g., a year is too long, integrated monthly data are near minimum). Third, the reliability of simplified models can often best be tested at longer time steps with data not originally required in the model (e.g., annual increments in stem biomass recorded over decades). Because the Landsberg and Waring model represents a formulation of the Light Use Efficiency model (Table 3.5) that provides for estimates of monthly allocation of NPP above and below ground, it has much wider potential application than other models and warrants comparison with data acquired for other life forms with different allocation patterns (Law and Waring, 1994). Moreover, because of the monthly time steps, the modified LUE model can be easily run with condensed averaged weather data and monthly estimates of the ability of the vegetation to absorb PAR.

C. Allocation Indices

A number of simple allocation indices can be distilled from our discussion on allocation. One is based on the idea that canopies can be assumed to respond to the total PAR absorbed in a linear fashion and that yield can be related directly to APAR under favorable environments. John Monteith first proposed this scheme and verified its application on crops (Monteith, 1977) and wet tropical forests (Monteith, 1972). He assigned the symbol epsilon (ε) to the amount of dry matter or its carbon equivalent produced above ground per unit of the annually absorbed PAR. Epsilon for crops and other vegetation that grow in well-watered and fertile soils usually has a maximum value of ~0.7 g C MJ^{-1} APAR (Monteith, 1977; Jones, 1992; Landsberg *et al.,* 1996). This maximum value, however, is rarely observed in forests, because of stomatal constraints associated with less than optimum conditions, and because of the increasing fraction of carbon allocated below ground in suboptimal environments. Across the Oregon transect, Runyon *et al.* (1994) reported that ε for aboveground NPP ranged from 0.09 to 0.46 g C MJ^{-1} APAR. On the other hand, when Light Use Efficiency was calculated by deducting that fraction of PAR absorbed when photosynthesis was limited by other environmental constraints, ε approached a constant for total NPP (above and below ground) of ~0.65 g C MJ^{-1} APAR. The original definition of epsilon (g NPP_A MJ^{-1} APAR) is valuable in judging the combined limitations that the environment exerts on photosynthesis and restricts growth allocation above ground, as will be shown in landscape and regional analyses presented in Chapters 8 and 9.

More specific allocation indices are also available; within a species, subtle shifts in carbon allocation may have diagnostic value. As noted, stem growth has relatively low priority in comparison to root growth. On the other hand, many secondary compounds, such as protective chemicals, are less essential than diameter growth because new foliage requires supporting sapwood. Because carbon allocation to stem wood reflects the carbon uptake per unit of foliage, and allocation below ground, the annual growth of stem wood per unit of foliage, termed "Growth Efficiency," is a general index of tree vigor that can help managers interpret the benefits of various silvicultural options and anticipate the response of forests and individual trees to attack by insects and pathogens (Chapters 5 and 6).

TABLE 3.5
Computation of Light Use Efficiency Conversion of Visible Radiation into Aboveground Net Primary Production and Net Ecosystem Production[a]

Input	Derived input	Equation	Prediction
Incoming solar radiation (I_s)	Photosynthetically active radiation (PAR)	PAR = 0.5 × solar radiation	PAR
Leaf area index (LAI) (with seasonal variation)	Fraction of PAR absorbed (FPAR) (*apply Beer's law*)	PAR × FPAR = APAR (MJ PAR m^{-2} $year^{-1}$)	Absorbed PAR (APAR)
Quantum efficiency (α; *function of chlorophyll content in canopy*)	max (α) ≈ 1.8 g C MJ^{-1} APAR (*decreases with reduction in chlorophyll content*)	$GPP_{pot} = APAR \times \alpha$	Potential gross primary production (GPP_{pot})
Temperatures, humidity, precipitation, and soil water storage capacity	Environmental constraints on photosynthesis	$GPP_{actual} = APAR \times \alpha f(H_2O)\, f(D)\, f(T)$ [Eq. (3.14)]	Actual gross primary production (GPP_{actual})
All the above inputs for Eq. (3.14)	GPP_{actual}	Net primary production (NPP) = $K_{(NPP/GPP)} \times GPP_{actual}$	NPP[b]
All the above inputs	Aboveground net primary production (NPP_A)	$NPP_A = f(GPP_{actual}/GPP_{pot})$ (see Fig. 3.16)	NPP_A[c]
I_s, LAI, NPP_A	Light Use Efficiency conversion (ε)	$\varepsilon = NPP_A/APAR$	ε[d]
Annual litterfall (LF) when litter accumulation on forest floor (FF) is near steady state	Net ecosystem production (NEP) Heterotrophic respiration (R_h)	Leaf litter, $R_h = f(LF/FF)$ [Eqs. (4.2) and (4.3)] Root litter $R_h = 0.5\,NPP_B$ (see Figs. 3.6 and text) $NEP = NPP - \Sigma R_h$	NEP[e]

[a]This table summarizes concepts and relationships presented in the text.
[b]The proportion of gross primary production converted into biomass (carbon) annually, $K_{(NPP/GPP)}$, is generally a conservative value within a biome, averaging 0.25 for boreal forests and 0.5 for temperate forests. Comparable data are not yet available for tropical forests.
[c]The annual ratio of aboveground to belowground NPP increases from 0.75 to 0.35 for forests as constraints on photosynthesis increase (GPP_{actual}/GPP_{pot}). Soil fertility also affects allocation but is incorporated in the amount of foliage present (LAI) and its chlorophyll content, which together determine FPAR and α.
[d]The light use efficiency conversion (ε) defined by Monteith (1972) ranges from a maximum of 0.7 to 0.1 g C MJ^{-1} APAR as conditions becomes less favorable for photosynthesis and aboveground growth (see Section VI,C on allocation indices).
[e]Net ecosystem production = $GPP_{actual} - R(\text{leaf litter})_h - R(\text{root litter})_h$. In Chapter 4, equations are presented that correlate annual leaf (and twig) litterfall with forest floor litter accumulation to estimate mean residence time of aboveground litter and the fraction of carbon (or mass) lost annually through heterotrophic respiration, $R(\text{leaf litter})_h$. Belowground heterotrophic respiration associated with root decay also can be estimated at steady state from measurement of annual litterfall with the equation presented with Fig. 3.6, assuming that the total belowground allocation of carbon is proportioned as 50% to NPP_B, 25% to autotrophic root respiration R_a, and 25% to $R(\text{root litter})_h$ (Ryan, 1991b).

The growth efficiency index is akin to the ratio of nonphotosynthetic tissue produced per mass of foliage (Briggs *et al.,* 1920; Burger, 1929) but expresses foliage in units of area rather than mass. This is an important distinction because the allometric relations are generally defined in units of mass to mass. If the same mass of leaves is distributed into more area, more light may be intercepted, but the total photosynthesis by the canopy may or may not be increased, depending on how nitrogen is distributed to chlorophyll pigments and the Rubisco enzyme. Alternative indices of growth efficiency have been calculated for other organs (Axelsson and Axelsson, 1986). When the referenced product has a special value, such as fruits, nuts, bark, or a specific wood product, the ratio of production to leaf area is termed a *harvest index.*

The pattern of structural growth changes with the availability of certain critical resources and with the imposition of specific kinds of physical stresses. For example, shoot extension on individual branches, as we might expect from analysis of photosynthesis, is closely related to the proportion of light intercepted and the availability of nitrogen (Dougherty *et al.,* 1994). It follows that more shaded branches export proportionally less photosynthate per unit leaf area. When the canopy of a tree is fully shaded, lower branches die and an umbrella-like canopy results (Steingraeber *et al.,* 1979; Kohyama, 1980). Root growth and seed production are also greatly reduced in plants growing in shade. These more subtle kinds of shifts in allocation have special diagnostic value that will be discussed in more detail in Chapter 6.

VII. COMPARISON OF FOREST ECOSYSTEM MODELS

There are now a score of models that integrate carbon, water, and elemental cycles into simulations of forest ecosystem behavior. Some models such as PGEN (Friend, 1995), MAESTRO (Wang and Jarvis, 1990), and MBL/SPA (Williams *et al.,* 1996) provide detailed simulations of instantaneous canopy light absorption and photosynthesis but are not complete ecosystem models. TREGRO (Weinstein and Yanai, 1994) explicitly models tree growth from carbon balance principles and the influences of atmospheric and nutritional stresses, but it does not incorporate a water balance nor allow for multidecadal changes in LAI and stand composition.

Where the objective is to simulate stand growth, many models incorporate only those variables that are important locally in limiting forest production. For example, the models TREEDYN3 (Bossel, 1996) and FORGRO (Mohren and Ilvesniemi, 1995) were developed for nutrient-limited European forests where water stress rarely limits growth. As a result, these models emphasize soil elemental cycles and nutrient limitations and largely ignore energy and water budgets. Similarly, the SPM model (Cropper and Gholz, 1993) incorporates many details of carbon uptake and allocation for slash pine forests that grow only in areas that do not experience drought. In contrast, Bonan (1993) emphasizes energy and water budgets in his simulation of boreal forest photosynthesis and productivity. The latter type of model partitions energy into sensible and latent heat components and thus is easily coupled to land-surface climate models (Bonan, 1995). A whole class of models developed to describe land–atmosphere interactions by the physical sciences and climate modeling community treats canopy energy, water, and carbon exchange with common sets of equations (Sellers *et al.,* 1996a).

Clearly, models that define only a limited but detailed set of variables can quite accurately predict the behavior of a restricted range of forest ecosystems. To extend predictions, more general ecosystem models such as GEM (Rastetter *et al.,* 1991) are required. These general models demand a number of simplifying assumptions to expand their range of application, and, in the process, they lose some accuracy. For example, the PnET model of Aber and Federer (1992) is based on only two principal relationships: (1) maximum photosynthetic rate is a function of foliar nitrogen concentration, and (2) stomatal conductance and transpiration are related to the actual photosynthetic rate. Rather than applying a sophisticated carbon allocation scheme to distribute NPP, the model constrains leaf growth by water availability, which in turn is correlated allometrically with fine-root growth, as the residual is partitioned into woody biomass. In spite of this simplified model structure and the use of monthly climate data, PnET was able to simulate NPP_A surprisingly well across a range of forest stands (see Fig. 5.20). Additionally, as will be illustrated in Chapters 7–9, these simplified models with minimal parameter requirements (such as the LUE model presented in this chapter) can be implemented across landscapes (Coops *et al.,* 1998), whereas models with detailed tree and stand data requirements cannot (Aber *et al.*, 1995).

A powerful approach to address the multiple levels of ecosystem complexity is a set of nested models linked by common logic. McMurtrie *et al.* (1992) applied the refined MAESTRO hourly canopy photosynthesis model to extract critical simplifications for the daily BIOMASS forest production model (McMurtrie and Landsberg, 1992). Properties extracted from BIOMASS were further distilled into a Generic Decomposition and Yield model, G'DAY (Comins and McMurtrie, 1993). The G'DAY model requires only 10 differential equations to represent tree and soil carbon and nitrogen dynamics over time. These three models were run sequentially to evaluate the effect of elevated atmospheric CO_2 on forest growth. Doubled CO_2 was predicted to increase leaf photosynthesis by 30–50% depending on air temperature, which might lead initially to a 27% increase in annual stand productivity. Eventually, however, changes in soil carbon and nitrogen were projected to limit N availability and result in a sustained increase in forest production of only 8%. No single model could apply to all the desired time scales. A common theoretical foundation, however, provided the means to seek and test simplifying assumptions derived from more detailed models. Once tested, the simplifying assumptions provided a basis for extrapolation into conditions for which no direct experimental data yet exist.

Forest biogeochemical models of general ecosystem processes can be applied to a wider range of vegetation than forests. All of the processes identified in Table 1.1 are shared by all terrestrial ecosystems. Consequently, a forest model such as FOREST-BGC has been modified to represent a grassland as BIOME-BGC by simply redefining certain canopy gas exchange and carbon turnover parameters (Running and Hunt, 1993). In a like manner, the CENTURY grassland model (Parton *et al.,* 1993) was redefined to simulate forest ecosystems and other broadly distributed terrestrial vegetation. The TEM model of McGuire *et al.* (1993) originated as a general multibiome biogeochemical model. TEM, CENTURY, and BIOME-BGC are useful in global biogeochemical simulations because they include common ecosystem processes in a logical framework and demand only a minimum amount of detail on stand and site characteristics (see Chapter 9). On the other hand, if provided detailed stand data, these models can also simulate forest productivity and other properties often as well as more specialized forest models.

The large variety of forest ecosystem models illustrates that selection of a model should carefully be matched with objectives. Models provide a versatile means to quantify how ecosystem processes may vary and affect forest growth and other properties. No single model, however, should be expected to apply to all situations, and, when supporting policy decisions, any specific model should be tested to assure its appropriateness to answer selected questions in an acceptably reliable manner.

VIII. SUMMARY

Carbon exchange from forest ecosystems represents a balance between uptake, storage, and losses. The upper limits on photosynthesis are set by the amount of photosynthetically active radiation absorbed by the entire canopy. The amount of radiation absorbed is a function of canopy LAI, chlorophyll pigments, and other related properties. Photosynthesis is the best understood of all ecosystem processes. Fundamental equations are available to describe the process, and models now predict rates close to those measured with eddy-flux analyses.

Autotrophic respiration is also a relatively well-understood process. By separately accounting for carbon content and synthesis cost of all components of NPP and the carbon expended in the maintenance of living cells, a forest carbon balance can be made. Such component analyses, combined with field experiments on plantations, have greatly increased our ability to interpret how changes in resource availability affect carbon allocation. A variety of conflicting theories on allocation exists, but a series of field experiments have greatly increased our understanding of the allocation process. This is fortunate because allocation is a key toward understanding competitive relations among species (Chapter 5).

Heterotrophic respiration is one of the most difficult processes to model, even with a detailed understanding of microbial biology, because microbial respiration takes place in a spatially heterogeneous environment. Carbon to nitrogen ratios or more refined indices that represent substrate quality are helpful, but these must be coupled to hydrologic models to predict seasonal variation in heterotrophic activity.

At present, we rely heavily on simple annual allocation indices related to the efficiency with which carbon is incorporated into biomass per unit of light absorbed (ε) or stem growth per unit of leaf area (growth efficiency), as general indices of stress. We still lack an adequate theoretical base for developing more general phenological models and must rely at present on empirical correlations with direct (or satellite) observations. A number of new indices look promising for improving our ability to predict seasonal allocation patterns under changing environments; in particular, the ratio actual GPP/potential GPP and the total canopy N content are candidates against which to test a variety of theories. The simplified models and indices presented in this chapter are the foundation for further extrapolations in time and space.